University of South Florida
Scholar Commons

Graduate Theses and Dissertations Graduate School

11-2-2007

Processing And Characterization Of Zinc Oxide Thin Films

Michael Depaz
University of South Florida

Follow this and additional works at: https://scholarcommons.usf.edu/etd

Part of the American Studies Commons

Scholar Commons Citation
Depaz, Michael, "Processing And Characterization Of Zinc Oxide Thin Films" (2007). *Graduate Theses and Dissertations.*
https://scholarcommons.usf.edu/etd/694

This Thesis is brought to you for free and open access by the Graduate School at Scholar Commons. It has been accepted for inclusion in Graduate Theses and Dissertations by an authorized administrator of Scholar Commons. For more information, please contact scholarcommons@usf.edu.

Processing And Characterization Of Zinc Oxide Thin Films

by

Michael Depaz

A thesis submitted in partial fulfillment
of the requirements for the degree of
Master of Science in Mechanical Engineering
Department of Mechanical Engineering
College of Engineering
University of South Florida

Co-Major Professor: Ashok Kumar, Ph.D.
Co-Major Professor: Jing Wang, Ph.D.
Muhammad Rahman, Ph.D.
Makoto Hirai, Ph.D.

Date of Approval:
November 2, 2007

Keywords: pld, sputtering, afm, xrd, resonator, nanoindentation

© Copyright 2007, Michael Depaz

TABLE OF CONTENTS

LIST OF TABLES iii

LIST OF FIGURES iv

ABSTRACT vii

CHAPTER ONE: BACKGROUND

1.1 Introduction 1
1.2 Piezoelectric Materials 3
1.3 Zinc Oxide 6
1.4 Resonators 8
1.5 Conclusion 12

CHAPTER TWO: SYNTHESIS OF ZnO THIN FILMS

2.1 Introduction 13
2.2 Plasma 13
2.3 Thin Films 14
2.4 Pulse Laser Deposition (PLD) 15
2.5 Sputtering 19

CHAPTER THREE: FILM CHARACTERIZATION

3.1 Introduction 24
3.2 X-Ray Diffraction 24
3.3 Atomic Force Microscope 28
3.4 Nanoindentation 30
3.5 Film Thickness Measurements 35
3.6 Normal Load Method 37
3.7 FTIR 39

CHAPTER FOUR: RESULTS AND DISCUSSION

4.1 Optimization of Pulse Laser Deposition (PLD) 40
4.1.1 Substrate Temperature Effects 42
4.1.2 O_2 Partial Pressure 46
4.1.3 Temperature Variations at 100 Millitorr 48
4.1.4 FTIR 50
4.1.5 Surface Roughness 51
4.1.6 Deposition Rates 54
4.1.7 Nanoindentation 55
4.1.8 Conclusion for the Optimization of PLD 58

4.2 Optimization of Sputtering Depositions 58
4.2.1 Argon to Oxygen Flow Rate Ratios 60
4.2.2 RF Power 62
4.2.3 Substrate Temperature Effect 64
4.2.4 Roughness 68
4.2.5 Deposition Rate 69
4.2.6 Conclusion of the Optimization of Sputtering Depositions 71

4.3 Calculation of the Piezoelectric Coefficient by the Normal Load Method 72

CHAPTER FIVE: CONCLUSION AND FUTURE WORK

5.1 Conclusion 76
5.2 Piezoelectric Response with the AFM 79
5.3 Resonator 81
5.4 Future of the Field 83

REFERENCES 86

LIST OF TABLES

Table 1.1 Piezoelectric Properties of Various Materials [10, 11, 15] 8

Table 1.2 Material Thickness 11

Table 3.1 ZnO Reference Values for ZnO 27

Table 3.2 Hardness and Modulus on Different Substrates [32] 35

Table 4.1 Experimental Conditions for the PLD 41

Table 4.2 XRD Analysis Based on Temperature Variations at 200 Millitorr 46

Table 4.3 XRD Analysis Based on Pressure Variations at 200°C 48

Table 4.4 XRD Analysis Based on Temperature Variations at 100 Millitorr 49

Table 4.5 Experimental Conditions for Sputtering 60

Table 4.6 XRD Analysis Based on Various Ar:O_2 Flow Rates 62

Table 4.7 XRD Analysis Based on Various RF Power Settings 63

Table 4.8 XRD Analysis Based on Various Temperatures 66

Table 4.9 Piezoelectric Coefficients 73

LIST OF FIGURES

Figure 1.1	Piezoelectric Effect [12]	4
Figure 1.2	Longitudinal and Transverse Piezoelectric Coefficients [13]	6
Figure 1.3	ZnO Crystal Structure [8]	7
Figure 1.4	Cantilever Beam Design	11
Figure 2.1	Schematic of the PLD System [19]	16
Figure 2.2	PLD Equipment Used in the Depositions	17
Figure 2.3	Plasma Formation from the Laser	18
Figure 2.4	Sputter System Used in Depositions	20
Figure 2.5	Plasma Formation in the Chamber	21
Figure 2.6	Argon Ions Impacting the Target	22
Figure 3.1	Bragg's Law [11]	26
Figure 3.2	ZnO Hexagonal Wurtzite Crystal Structure [11]	27
Figure 3.3	AFM Tip [26]	28
Figure 3.4	AFM Piezoresponse Schematic [28]	29
Figure 3.5	Compliance Curve [31]	32
Figure 3.6	Indenter Thin Film and Substrate Interaction [31]	34
Figure 3.7	Illustration of Warping of a Substrate	36
Figure 3.8	Schematic of Normal Load Method [34]	38
Figure 4.1	O_2 Pressure Varied at 300ºC	43

Figure 4.2	Temperature Varied at 200 Millitorr	45
Figure 4.3	ZnO Grown at 200ºC at Various Pressures	47
Figure 4.4	Temperature Varied at 100 Millitorr	49
Figure 4.5	FTIR Results	51
Figure 4.6	PLD Surface Roughness	52
Figure 4.7	3-D View of the Surface Topography	53
Figure 4.8	Surface Roughness	53
Figure 4.9	Deposition Rate at Various Temperatures	54
Figure 4.10	Deposition Rate at Various Pressures	55
Figure 4.11	Hardness	56
Figure 4.12	Modulus	57
Figure 4.13	Various Ar:O_2 Flow Rates	61
Figure 4.14	Various Power Settings	63
Figure 4.15	Temperature Variations	65
Figure 4.16	300°C Sample	67
Figure 4.17	Sputtering Surface Roughness	68
Figure 4.18	Deposition Rate at Various Ar % Flow Rates	69
Figure 4.19	Deposition Rate at Different Power Settings	70
Figure 4.20	Deposition Rate at Various Temperatures	71
Figure 4.21	Experimental Equipment	75
Figure 5.1	AFM Results of Films Piezoelectric Effect	80
Figure 5.2	First Mode of Vibration	82

Figure 5.3	Second Mode of Vibration	83
Figure 5.4	ZnO Nanowire Array	85

Processing And Characterization Of Zinc Oxide Thin Films

Michael Depaz

ABSTRACT

Zinc oxide is a very versatile material that can be used in many microsystems and MEMS applications. ZnO thin film has been utilized in a wide variety of MEMS devices because of its unique piezoelectric, optical, and electrical properties. In particular, piezoelectric property of ZnO can be used in numerous applications from resonators and filters to mass sensors and micro-actuators (e.g., micro-valve and micro-pump). Because of its versatility, this research was focused on analyzing some key properties of ZnO thin film achieved by two different deposition techniques, Pulsed Laser Deposition (PLD) and Sputtering. Multiple experiments were conducted in order to identify the best conditions for the growth of ZnO thin film. Under the optimum conditions, the ZnO thin films will provide the best piezoelectric performance in devices such as microcantilevers.

In order to find the best deposition conditions in both PLD and Sputtering multiple depositions have been done and then analyzed using the XRD, AFM, FTIR, nanoindenter, and ellipsometer. For the PLD the best conditions were found to be at 200°C with a partial pressure of O_2 of 100 millitorr. For the sputtering system the best film formed when the substrate temperature was kept at 400°C along with RF power of 250 Watts, and a flow rate of 25% O_2 and 75% Ar. Both experiments were similar in the

fact that both a certain amount of O_2 in the chamber and an elevated temperature are needed to facilitate the formation of ZnO crystal structure.

CHAPTER ONE: BACKGROUND

1.1 Introduction

The study of zinc oxide (ZnO) material and its employment in micro-scale and nano-scale devices has grown tremendously during the last decade. Zinc oxide is a very versatile material that can be used in many microsystems. The combination of its wide band gap, piezoelectric, electrical, and optical properties makes ZnO unique and crucial for a wide range of present-day and future device applications. Due to its high electromechancial coupling coefficient, ZnO is one of the leading candidates for efficient signal transduction between electrical and mechanical domains in both sensors and actuators. Needless to say, the recent development of nano-scale ZnO structures such as nanobelts, nanorods, and nanowires has spurred new vigor into its future implementation. Furthermore, ZnO also stands out from other materials because of its ability to operate in extreme conditions such as nuclear reactors and space, due to its better radiation hardness than most of other materials [1].

In particular, the piezoelectric characteristics of ZnO make it an outstanding transducer material for making MEMS resonators and mechanical switches. These small resonators are useful in wireless communication systems where small size, low power

consumption and the ability for on-chip integration with the microelectronics are greatly appreciated [2]. Piezoelectrically-actuated resonators in bulk acoustic wave (BAW) mode have been widely used in wireless communicators in frequency range between 1GHz to about 10GHz proving piezoelectric MEMS resonators can succeed in wireless world. Future wireless applications for such devices include reference oscillator with better stability and front-end filters with better selectivity [3].

Another application of ZnO piezoelectric effect is employed in mass-sensitive sensors, which are based on the acoustic wave phenomena. These transducers can be used for chemical and biological monitoring and operate in a similar fashion to the bulk acoustic wave devices in that the device resonates at its resonance frequency which is strongly dependent on the amount of external mass attached to the resonator. Therefore, when there is a mass-loading effect on the bulk acoustic wave resonator the frequency changes and the mass that is loaded on the device can be accurately measured [4].

Zinc oxide also has strong potential for nanotechnology, offering several key advantages over other materials. ZnO has a large band gap and excitation binding energy [5,6]. It also has useful piezoelectric characteristics, which makes it useful in making nano-scale electromechanical coupling devices such as nano-scale sensors and actuators [8]. ZnO is also a bio-compatible material and therefore can be used for many biomedical applications such as biomedical implants and coatings [9]. Aside from sensors and actuators, ZnO also provide some interesting luminescent properties. It can be made into nanorods and nanowire, which have short wavelength optoelectronics characteristics that can lead to a next-generation laser source operating in the ultraviolet range [5,7]. A great deal of research is going into the development and implementation of ZnO

nanostructures. Currently ZnO can be formed into nanorods, nanobelts, nanowires, nanocombs, disks/rings, nanosprings and nanopropellers to name a few [5, 6, 7, 8, 9]. Nanorods have some optoelectronics characteristics that may lead to its usage as an ultraviolet laser [7, 8]. Nanobelts can be used as very sensitive nano size gas sensors, nanoresonators, nanogenerators, and nanocantilevers [5, 6, 7, 8, 9].

ZnO is obviously a very versatile substance that can be used in microsystems applications as well as nanosystems. The study of ZnO and everything that it has to offer is a growing research field. Some of the micro-scale devices like the micromechanical resonators are in its infancy as far as what can and will be done. Recent development of microcantilevers demonstrate that piezoelectric resonators have strong potential and a lot of room for improvement. The nano size architecture of ZnO is still being investigated, so some the potentials of ZnO are still yet to be discovered.

1.2 Piezoelectric Materials

The piezoelectric affect was first discovered in 1880 by two brothers, Pierre Curie and Paul-Jaques Curie. They found that when a force was applied to certain crystals a charge was generated on the surface, and that the charge was proportional to the applied stress on the crystal [10, 11]. One year later they discovered that the opposite also proved to be true, an applied voltage would cause the crystal to deform, and likewise the deformation was proportional to the voltage applied. Piezoelectric materials got their name from the Greek word “Piezo” which means “press” [10].

There are a total of 32 possible crystal structures known for all materials, and of these 32 structures 20 of them exhibit piezoelectric properties. In order for a crystal to be a piezoelectric its structure cannot have a center of symmetry along at least one of its axis. This means that the atomic structure when perceived along a particular axis is different in structure along its opposite direction [11]. In a piezoelectric crystal the center of negative charge is located at the center of the crystal, and by exerting a force along an axis of non-central symmetry the crystal experiences a distortion. This distortion causes the center of mass of the central atom and the center of charge to be different from each other. As a result it creates an electric dipole in the structure [8].

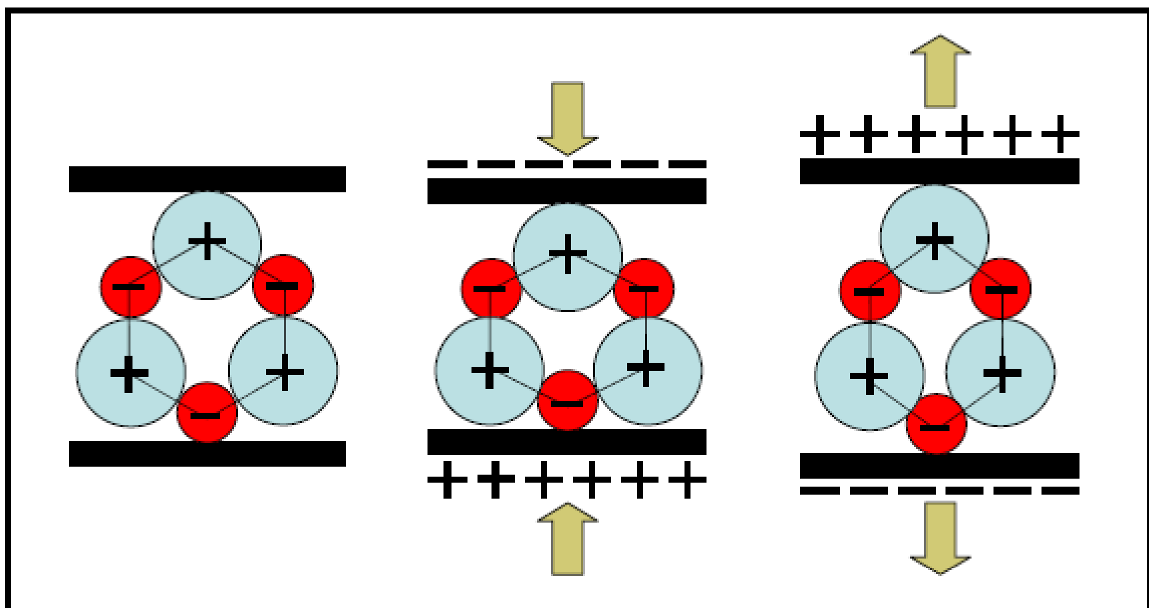

Figure 1.1 Piezoelectric Effect [12]

Since the strain on the structure causes anions (negative charge) and cations (positive charge) to move in opposite directions this forms an electric potential. When an electric current is applied to the crystal the cations and anions also move in opposite

directions causing the crystal to strain. Piezoelectric materials, therefore, can be strained by one of two methods, mechanically or electrically [10].

The piezoelectric formulas are related to charge equations of electrostatics by adding a piezoelectric constant [11]. The basic linear equation for the direct piezoelectric effect is.

$$D = Q/A = dT$$

Where D is the dielectric displacement, which is equal to the charge per unit area or Q/A. The piezoelectric constant d is in Coulombs per Newton and T is the stress.

The basic equation for the inverse effect is.

$$S = dE$$

Where S is the strain, E is the electric field and the piezoelectric constant d is in meters/Volt [11, 13].

A piezoelectric material can be deformed in multiple dimensions, giving various modes of applications. Since there are multiple axes that the crystal can be deformed on with non-central symmetry there are various piezoelectric coefficients that a material can have based on which axis is deformed. Figure 1.2 from B. Xu’s paper clearly illustrates the orientation dependence of the piezoelectric coefficient [13].

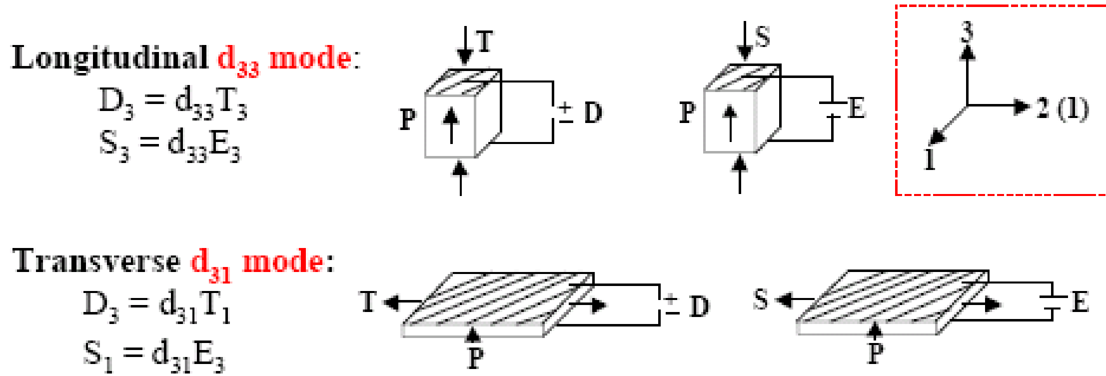

Figure 1.2 Longitudinal and Transverse Piezoelectric Coefficients [13]

This natural effect that occurs in 20 crystal structures can be used in making things like igniters for lighters, frequency filters, mass sensors, resonators, accelerometers, and the list goes on. This is why there has been tremendous interest in employment of these materials in MEMS applications.

1.3 Zinc Oxide

Zinc oxide is a piezoelectric material that has a hexagonal Wurtzite crystal structure. This structure, in order for it to be a piezoelectric material, of course, does not have central symmetry. ZnO has normal dipole moments and spontaneous polarization along the c-axis as seen in figure 1.3 [11]. Since ZnO has a strong piezoelectric effect in the c-direction, films with a high c-axis orientation are desired. These thin films show the best piezo activity when the c-axis is orientated perpendicular to the surface of the substrate. In order to achieve the proper orientation the film needs to be grown in the

(002) direction [10]. One of the advantages of ZnO is that it naturally grows in this direction in both the PLD and Sputtering when the substrate is heated.

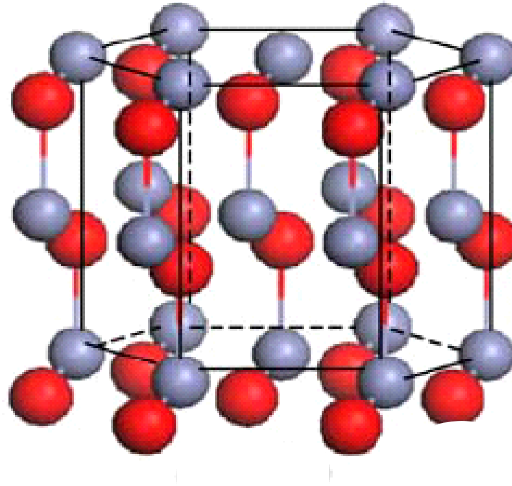

Figure 1.3: ZnO Crystal Structure [8]

Zinc oxide does not have the best piezoelectric coefficient compared with other piezoelectric materials like PZT (lead zirconate titanate) and $BaTiO_3$ (barium titanate), however ZnO does offer several advantages. It has both semiconductor and piezoelectric characteristics, it is also bio-safe and bio-compatible, and it also has found numerous applications in the nano-sciences due to the recent development of fabrication process for making diverse nanostructures [9]. It also stands out from other materials because of its ability to operate in extreme conditions such as nuclear reactors and space due to its better radiation hardness than most of other materials [1]. In addition, ZnO also features some interesting optical properties, which results in development of a UV laser based on ZnO material as well as ongoing research to explore the use of ZnO as a UV LED [14].

Table 1.1 Piezoelectric Properties of Various Materials [10, 11, 15]

Material	Piezoelectric coefficient	pC/N or pm/V
ZnO	d33	12.4
	d31	-5.0
	d15	-8.3
PZT	d33	117
AlN	d33	5.10
	d31	2.6
$BaTiO_3$	d15 (single crystal)	587
	d15 (polycrystalline ceramic)	270

1.4 Resonators

Piezoelectric zinc oxide can be used as structural material for micromechanical resonator enabled by Micro Electrical Mechanical Systems (MEMS) technologies. MEMS resonators are small micro-scale or nano-scale structures made in piezoelectric material. And such resonators simultaneously utilize the direct or inverse piezoelectric transduction in order to convert the signal between electrical and mechanical domains. Based on the direct piezoelectric effect, the resonator acts like sensor, when the structure is strained it produces a voltage and the amount of voltage produced is related to the amount of strain applied on the structure. This is how an inertia sensor such as an accelerometer works it determines a g force based on the amount of voltage produced by the piezoelectric material. Based on the inverse piezoelectric effect, the resonator acts like an actuator, when a AC voltage at the resonance frequency is applied across the built-in piezoelectric thin film, it causes the resonator to vibrate in its designed resonance mode and frequency. Obviously, a piezoelectric MEMS resonator is a unique transducer

that seamlessly integrates sensor and actuator components together which has gradually attracted more and more attention from the research community.

MEMS resonators have a variety of applications like frequency generators, filters, and sensors [16]. The telecommunication industry is the largest consumer of piezoelectric resonators demanding billions of bulk acoustic wave (BAW) filters annually. Most of them have been used in cell phones and base stations. Resonators can also be found in medical equipment for detection of various chemicals as well as in the automotive industry as tire pressure sensors. Other applications for them include vapor, humidity, and mass sensors [11]. As can be seen there are many applications for this kind of MEMS devices due to their several advantages. The wide acceptance of such MEMS resonators can be traced back to their excellent electromechanical coupling coefficient, lower power consumption, smaller size, and easier integration with integrated circuits, which suggests them the best option for the portable gadgets. The old adage "you get what you pay for" in this case, does not exactly apply; these devices even though they are relatively inexpensive give excellent performance and can be very reliable [16].

A typical cantilever beam resonator can be made by sandwiching ZnO with a top and bottom electrodes normally made out of aluminum or platinum. The top and bottom electrodes are needed, because they supply the input voltage needed to generate strain in the structure while detecting the induced output voltage. The input voltage is applied at a frequency similar to the natural resonance frequency of the cantilever in order to excite the device into its resonance vibration. When resonance occurs it amplifies the deflection of the cantilever beam which then results in stronger output voltage due to the inverse piezoelectric effect [2].

The layer dimensions can vary from one design to another but typically the top and bottom electrodes should be a few hundred nanometers thick, and the thickness of the piezoelectric layer stays between a few hundred nanometers and a micrometer. Table 1.2 shows the material dimensions used in the resonator simulation and Figure 1.4 shows the cantilever resonator design. The electrode thickness can have a significant effect on the natural resonance frequency [17]. Since the electrodes are simply there for providing or collecting the electrical charge, they can only affect the resonance vibration by applying additional mass to the structure and stiffening the secondary moment of inertia [17].

Several other factors also affect the performance of piezoelectric resonators. First, the anchor stiffness might have an influence on the resonance frequency. Second, the anchor is also a point where the mechanical energy can dissipate to the substrate thus leading to energy losses and lowering the quality factor (*Q*) of the device defined in the following equation [17]. Third, the aspect ratio, or the length to width ratio, is another factor that can affect the resonators characteristics. Previous research has suggested a higher aspect ratio will result in a higher quality factor (*Q*) and lower motional resistance due to the less energy losses and larger transducer area [17]. The quality factor equation is shown below.

$$Q = 2\pi * \text{Energy stored per cycle} / \text{Energy dissipated per cycle}$$

Table 1.2 Material Thickness

Film Material	Thickness (nm)
Pt (top electrode)	300
ZnO	500
Pt (bottom electrode)	300
Air Gap	2000
SiN	200
Si	10000

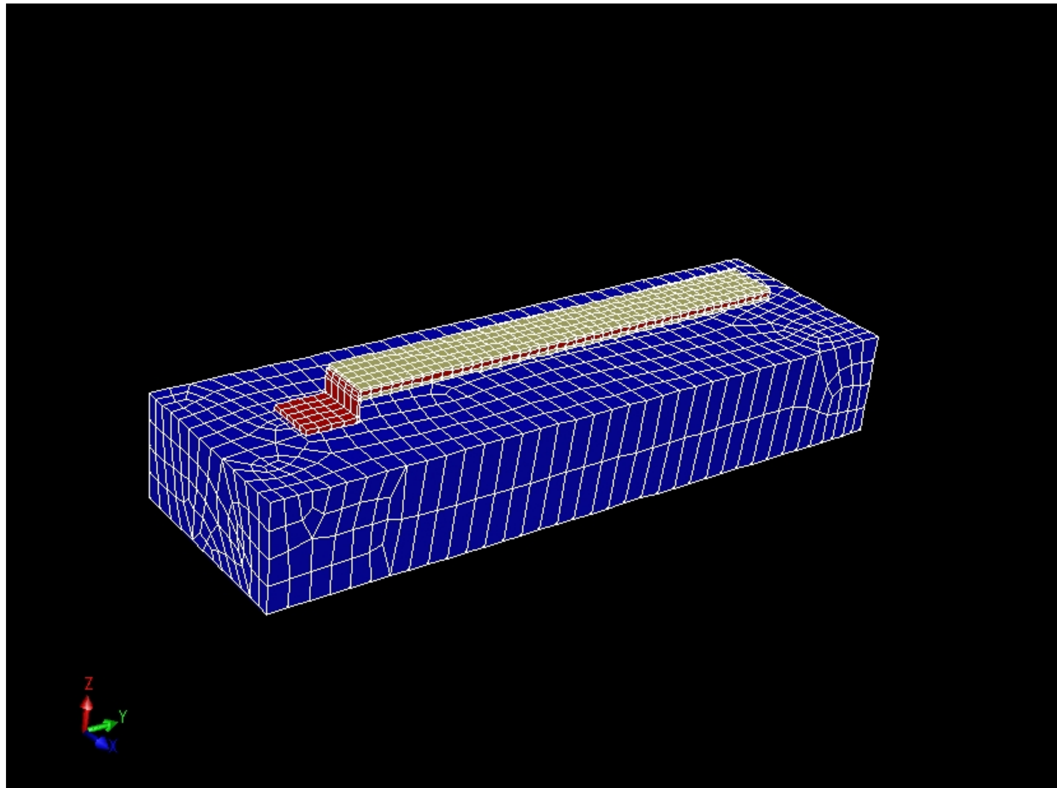

Figure 1.4 Cantilever Beam Design

1.5 Conclusion

Zinc oxide is a very useful material that can be employed in a wide variety of applications. Its piezoelectric characteristics make it a crucial transducer material in MEMS devices such as sensors and actuators. Particularly, the recent implementation of piezoelectric MEMS resonators into billions of wireless communication handsets has spurred new vigor into further development and optimization of the ZnO piezoelectric resonators. Besides its piezoelectric characteristic, ZnO also offers outstanding optical, electrical, and semi-conducting properties which makes it a unique and versatile functional material. Since MEMS and especially nanotechnologies are relatively new, there is a lot to be done, and many potential applications of the of zinc oxides have yet to be discovered. In the subsequent chapters, ZnO will be further examined as a functional material for making piezoelectric resonators.

CHAPTER TWO: SYNTHESIS OF ZNO THIN FILMS

2.1 Introduction

Physical Vapor Deposition (PVD) is how the ZnO thin films were deposited in this research work, so in the following two sections some basic information will be given on what plasma is and how it relates to PVD along with some information on thin films in general and their deposition techniques. After reviewing the basics on thin films and plasma, these sections will also provide background information on Pulsed Laser Deposition (PLD) and Sputtering which are the two chosen techniques for synthesis of ZnO thin film.

2.2 Plasma

There are four states in which matter can be found, including solid, liquid, gas and plasma. Plasma itself has been around since the dawn of time and has been seen in things like the Aurora Borealis, lightning, and the solar corona. Even though plasma has been seen in nature for this length of time, it didn't get an official name until Irving Langmuir

coined the term in 1929. Langmuir used the term to describe what happens to the gas when a high current is introduced in a vacuum tube [18].

Plasma is basically ionized gas that emits light when there is enough energy in the system to allow the molecules to split into individual ions. The light is seen because of the electrons within the atoms jump to different orbitals, when this happens a photon is produced creating the light. The transformation of a basic gas into a plasma or ionized gas is dependent on the energy introduced into the system and the gas pressure [18]. Typically a higher pressure environment requires more energy to create plasma. Plasma can be produced at atmospheric pressures, which is what happens when lightning strikes. However the energy of a lightning bolt is on the order of mega joules that is many order of magnitude higher than the 200 millijoules of energy, at which is the PLD operates.

Plasma is a related subject matter to this research because it is generated in both techniques used for ZnO thin film deposition (i.e., Sputtering and Pulsed Laser Deposition). Both Sputtering and Pulsed Laser Deposition are categorized as Physical Vapor Deposition (PVD) techniques. In the PVD process plasma is created in the chamber to remove material from the target, the target material ionizes in the chamber and then recombines onto the substrate [18].

2.3 Thin Films

Thin films are basically any kind of material layer with a thickness on the order of a few atoms to a few micrometers. Thin films are not a new technology; in fact they can be

seen as far back as 1500 B.C. where decorative gold leaf artwork was found from ancient Luxor, the artwork had gold with a thickness of about 0.3 μm [18]. Even though thin films are not a new technology they have only recently found their way into scientific and commercial applications.

A lot has changed since ancient Luxor, thin films are now being made out of virtually every material imaginable for a variety of applications. These applications be traced back to coatings that can provide items in micro-scale to macro-scale with wear and corrosive resistance. More recently, thin films have also been widely employed based on their other electrical, mechanical, optical, and thermal properties as well. Thin films are grown by depositing atoms onto the substrate surface and by altering the experimental conditions that affects the film's characteristics. Parameters such as the substrate temperature, energy, and chamber pressure can have an effect on the film's growth, deposition rate, and growth orientation.

2.4 Pulsed Laser Deposition (PLD)

There are many different ways in which ZnO can be deposited onto a substrate material like silicon, one such method is Pulsed Laser Deposition (also known as PLD). This method uses laser light energy to strike a target material to create a plasma.. The substrate is positioned in front of the target so the plasma plume hits the substrate. The ions in the gas can then form a thin film onto the substrate. Even though the basic idea of the PLD system seems easy, the theoretical aspects of the process are still not fully

understood [14]. Due to the lack of theoretical model, thin films are normally deposited under various conditions and then characterized to find the best deposition conditions.

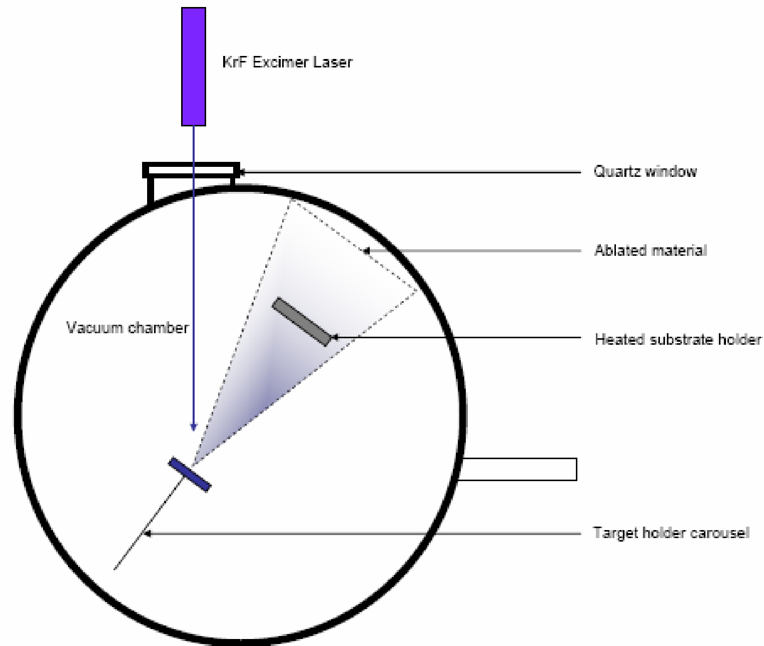

Figure 2.1 Schematic of the PLD System [19]

Before a deposition can be done the stainless steel chamber has to be evacuated by a basic mechanical pump, also known as roughing pump, from atmospheric pressure to several millitorr. Once evacuated a turbo molecular pump is turned on to further reduce the chamber pressure to 10^{-6} torr. The chamber is pumped down to ultra low pressure to remove all unwanted particles in the atmosphere to prevent contamination from any particles other than those desired to be ionized and deposited onto the substrate.

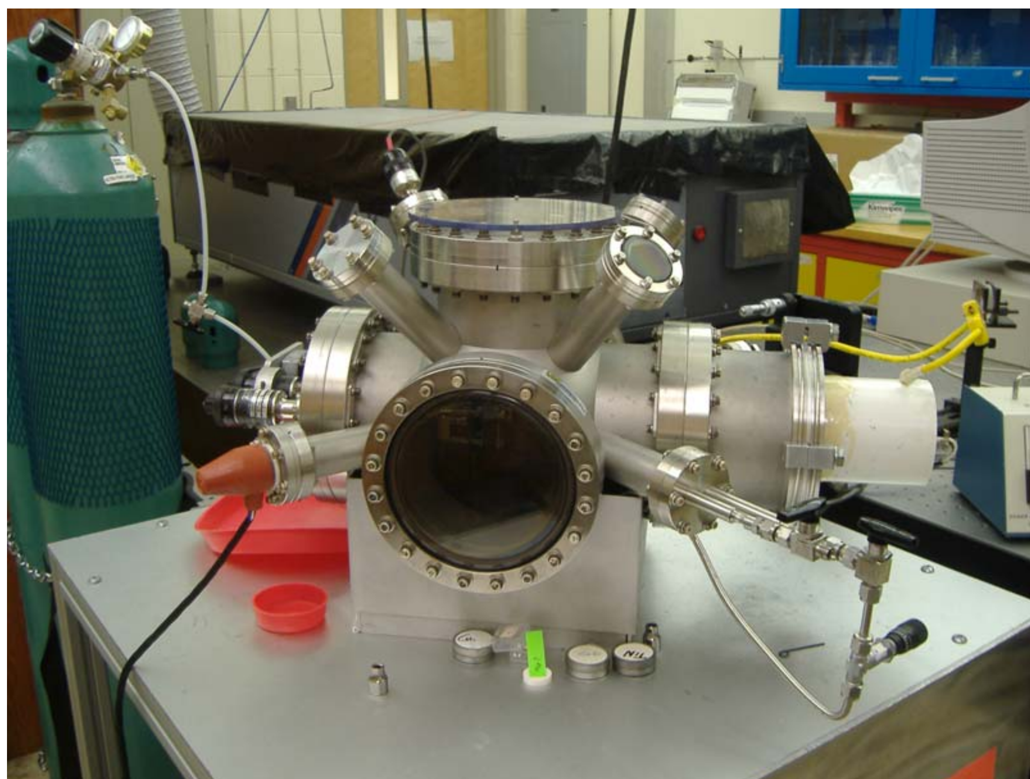

Figure 2.2 PLD Equipment Used in the Depositions

Once the chamber is pumped down either the deposition takes place in the vacuum or a reactive gas is added to react with the target material that is ablated off. For example when making an oxide, oxygen can be added to the chamber to facilitate the film recombination onto the targeted substrate as an oxide [5, 20]. The complication in adding a partial pressure is that it interferes with the mean free path of the particles. Having more ions floating in the chamber interferes with those that are ejected from the target and therefore reduces the deposition rate. So when adding a reactive gas to the chamber one must add just enough gas to ensure that it force the reaction to occur, but not too much as to drastically reduce the mean free path of the particles thus lower the deposition rate.

The substrate temperature is another factor that affects the formation of the thin film. Heating the substrate gives energy for the formation of a crystal orientation in the

film being deposited [14]. If there isn't enough thermal energy present in the system then the film deposited might become polycrystalline instead of the desired monocrystalline. On the other hand, if there is too much heat then the film may become rough or have too much residual stresses.

Once the desired experimental conditions are reached, then the KrF laser is switched on to ablate material off of the rotating target. The laser is pulsed at a frequency of 10Hz and delivers 200mJ to the target at a wavelength of 248nm.

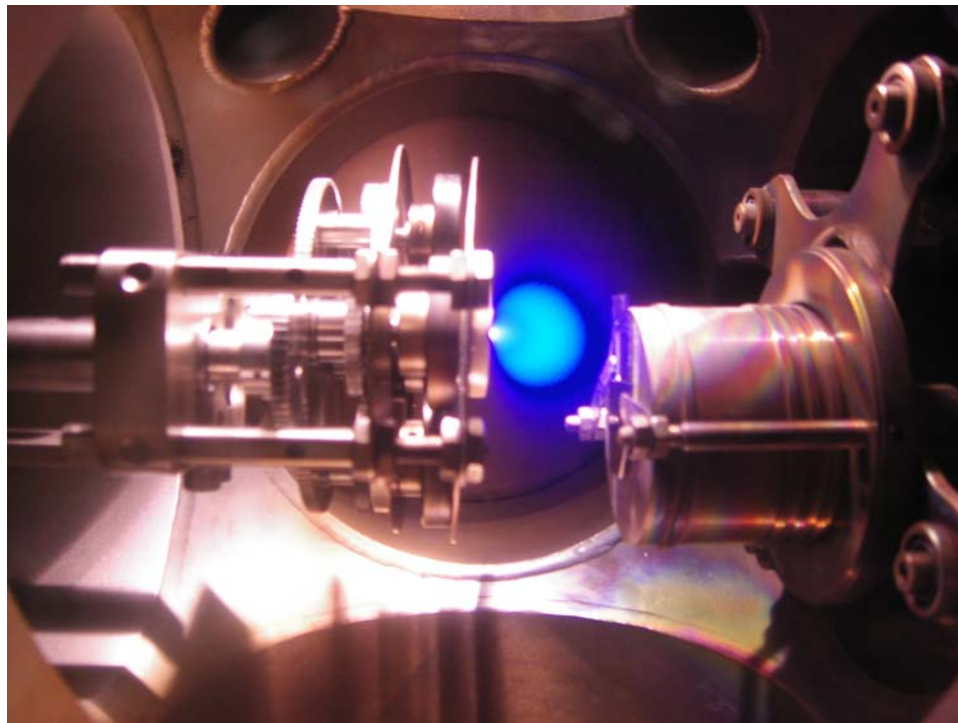

Figure 2.3 Plasma Formation from the Laser. Picture by Dr. Makoto Hirrai

As can be seen from Figure 2.3 the plasma plume hits the substrate material in a direct path, because of this, the substrate needs to be positioned directly in front of the target in order for the particles in the plasma to recombine onto the substrate. The distance between the substrate and the target also influences the deposition rate. The

closer the substrate is to the target and the more energetic the plasma is, the more particles can be deposited onto the substrate.

2.5 Sputtering

Sputtering is in fact a very similar process to the PLD, it is also characterized as Physical Vapor Deposition process that uses plasma in the chamber to physically deposit a thin film. Other similarities to the PLD system lie in the fact that the substrate is heated, a reactive gas can be added into the chamber, and the amount of pressure in the chamber also affects the deposition rate. Despite these similarities, Sputtering is a very different process, where the plasma forms in a different manner. The plasma is formed in the chamber by using a radio frequency or RF power source to ionize argon gas, which is being passed through the chamber.

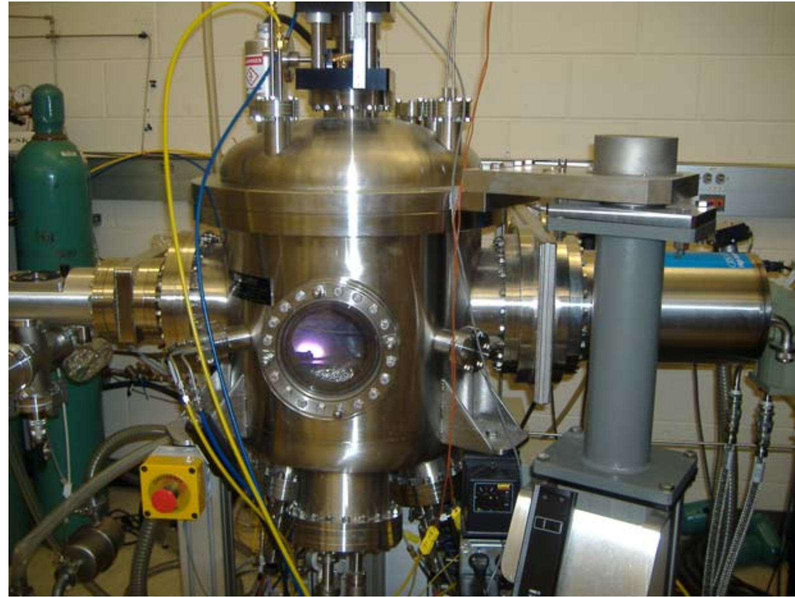

Figure 2.4 Sputter System Used in Depositions

Before going further into further details, the process will be described in layman-terms. This will help the readers to envision what is happening. Everyone must have seen an action movie at one point or another, well in an action movie whenever someone shoots a gun and the bullet hits the ground you see dirt fly into the air. This is analogous to what happens in the Sputtering chamber. The energized argon ions are like lead bullets, and the ground is like our target in the chamber. When the argon ions hit the target it ejects material just like when the bullet hits the dirt. Now if we put a piece of tape over the ground where the bullet hits, every time a bullet impacts the ground the tape will capture some of the dirt that flies in the air. The heated substrate is like the piece of tape collecting the target material, and of course going one step further with this analogy the more bullets that hit the ground, the greater amount of dirt can be thrown into the air and the closer in succession that those bullets hit the dirt the faster that piece of tape can become covered with dirt.

The process uses high-energy ions to bombard or “sputter” material from the target to the substrate. The target is negatively charged and the substrate is grounded, this is done so that the argon ions are drawn to the target and thereby sputter the target off [11]. Since Sputtering occurs due to the ions hitting the target, the deposition rate is dependent on the number of ions that bombard the target in a given time [18]. The higher the power setting is the faster the deposition rate is. A high power setting would be like using a machine gun to hit the target versus a typical gun. This method, as can be visualized, also requires that the target and the substrate be in direct line of site with each other [10].

Figure 2.5 Plasma Formation in the Chamber

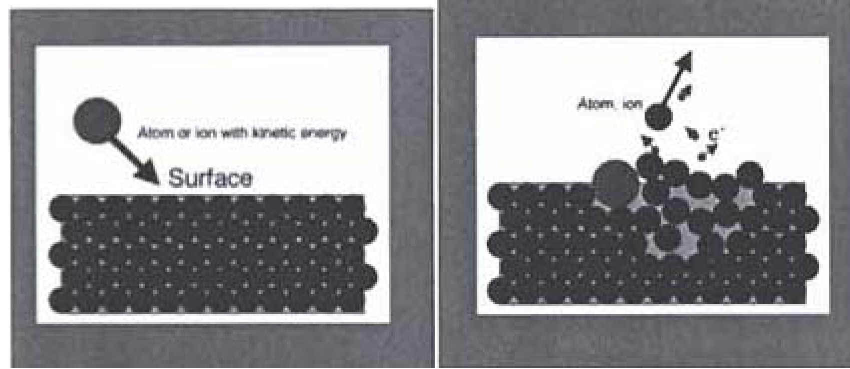

Figure 2.6 Argon Ions Impacting the Target. Figure from Micro and Nano Manufacturing class notes, by Dr. Ashok Kumar

There are several parameters that can affect the film's quality and deposition rate, these parameters are RF power, the substrate temperature, chamber pressure, reactive gas to argon ratio, and the distance between the target and the substrate. As mentioned before, a higher power setting will give a faster deposition rate. Heating the substrate, like in the PLD system, gives energy for the formation of a crystal in the film being deposited [14]. The closer the target is to the substrate the more of the target material ejected from the target hits the substrate, giving a better deposition rate.

Adding a reactive gas to the chamber while Sputtering is called reactive Sputtering and is typically used when deposition something like an oxide. In the case of depositing zinc oxide, oxygen is added to the chamber to facilitate the formation of the ZnO on the substrate. When ZnO molecules leave the target they decompose into zinc and oxygen ions, sometimes the zinc does not recombine with the oxygen before it reaches the substrate, depositing more zinc than there should be [10, 21]. In the deposition of ZnO a crucial parameter is finding the right ratio between argon and oxygen that needs to be applied to the chamber to get the best results. Too much oxygen will help in forming the oxide film, but will reduce the amount of argon that can be used to

bombard the target. On the other hand, having not enough oxygen could lead to excess zinc in the thin film.

The chamber pressure is another factor that affects the deposition rate. The greater the pressure is the lower the mean free path of the particles is. This means that with a higher pressure the particles that are traveling to the substrate collide with each other more frequently and as a result some of the particles will be scattered back to the target or some other directions away from the substrate [10]. The mean free path therefore affects the deposition rate. A lower pressure is therefore desired for achieving a better deposition rate, the problem is that in the Sputtering system unlike the PLD a certain amount of argon must be present to generate the plasma in the chamber. Having too much pressure in the chamber will lead to a lower deposition rate because it affects the mean free path, but having too low of a pressure reduces the amount of argon atoms that hit the target and as a result also lowers the deposition rate.

Sputtering requires several experiments to identify what the best conditions are to deposit films of desired quality. It is a big balancing act in finding the best argon to oxygen ratio, the best chamber pressure, and identifying the appropriate substrate temperature, and power setting.

CHAPTER THREE: FILM CHARACTERIZATION

3.1 Introduction

After ZnO thin films have been deposited by various techniques already mentioned, they must then be analyzed by a variety of methods to determine material characteristics the film has. The methods that are used include X-Ray Diffraction, Atomic Force Microscopy, Nanoindentation, FTIR, Profilometry, and Ellipsometry.

3.2 X-Ray Diffraction

X-Ray Diffraction (XRD) is a useful method that is used to analyze a materials crystal structure. X-rays are used because of their small wavelength, which is on the order of angstroms, radiation at this wavelength is small enough to go in between adjacent atoms and hit multiple planes in the crystal structure [22]. The incoming x-rays hit the surface. The interference from the constituent atoms in the crystal causes the x-rays to scatter. It is the scattering of these waves from the different planes of the atomic structure that gives us a diffraction pattern. Since a diffraction pattern is related to how the x-rays hit and interfere with the planes of the crystal structure, if the planes of the crystal are

orientated in a different direction it will yield a different diffraction pattern. Patterns are directly correlated to unique crystal structures [11].

The diffraction patterns obtained through the XRD method can give a variety of information about the material like crystallite thickness, the interplanar spacing of the structure, orientation of the crystal or crystals in the film, and if there are any residual stresses in the film. This is all done by looking at the peak position and its shape [10]. To calculate the interplanar spacing of the crystal we use Bragg's Law [10, 11, 22]:

$$2d\sin\theta=n\lambda \text{ or } d= n\lambda/2\sin\theta$$

Where d is the distance between lattice planes, θ is the scattering angle, n is the order of diffraction peak, and λ is the wavelength of the x-rays (typically 1.54Å). By observing the distance of the interplanar spacing we can see if the film is under stress and whether it is compressive or tensile. If the peak position is slightly less than the know diffraction angle then the interplanar spacing will increase meaning that the film is under compressive forces, and like wise if the peak position is slightly more than the know diffraction angle then the film will be under tension. Figure 3.1 shows how the different x-ray waves interact with the surface atoms. It also shows where Bragg's Law comes from.

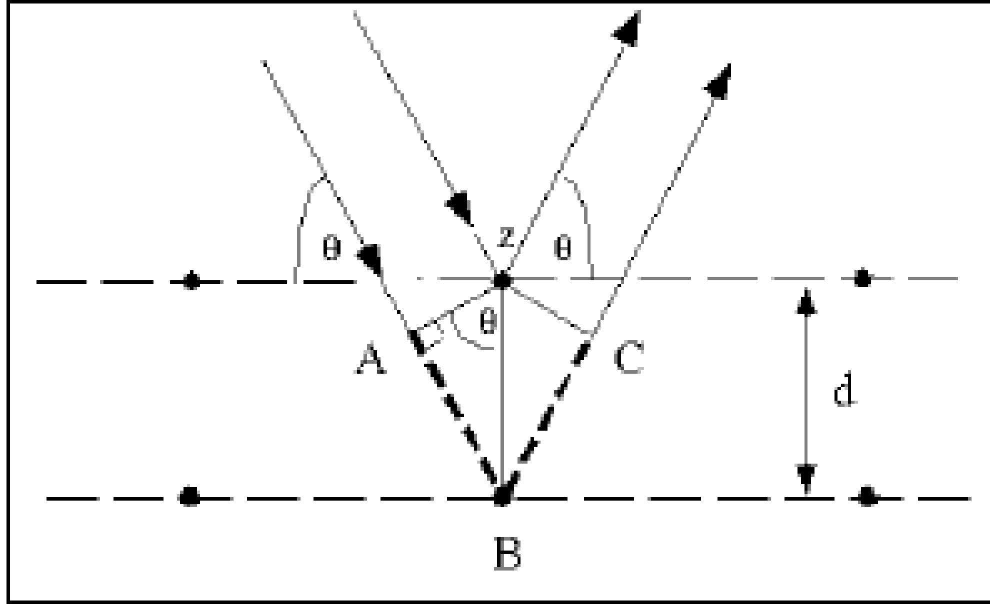

Figure 3.1 Bragg's Law [11]

When performing X-Ray Diffraction to look at a crystal the optimum diffraction pattern would be a single peak, high intensity, and very narrow. The narrow peak means that the whole structure is a single crystal with one orientation. This, however, rarely or never happens typically the peak has a certain width, this width shows that the film has grains or crystallites in it. By using Scherrer's equation the crystallite thickness can be calculated [23]. Scherrer's equation is:

$$tB\cos\theta_B = k\lambda \quad \text{or} \quad t = k\lambda / B\cos\theta_B$$

where t is the crystallite thickness, k is a constant equal to 0.89, θ_B is the Bragg angle, λ is the x-ray wavelength, and B is the full width at half max value.

Low film stress is critical in making a cantilever resonator out of any piezoelectric material [24]. The XRD results that are desired for making a good ZnO piezoelectric film is to have a crystal orientation of (002) this occurs at an angle of 34.422 ˚ [10].

Table 3.1 ZnO Reference Values for ZnO

Crystal Structure	Hexagonal
hkl crystal orientation	002
2θ	34.420
d-interplanar spacing	2.6033 Å
c-direction spacing	5.20661 Å
a=b	3.24982 Å

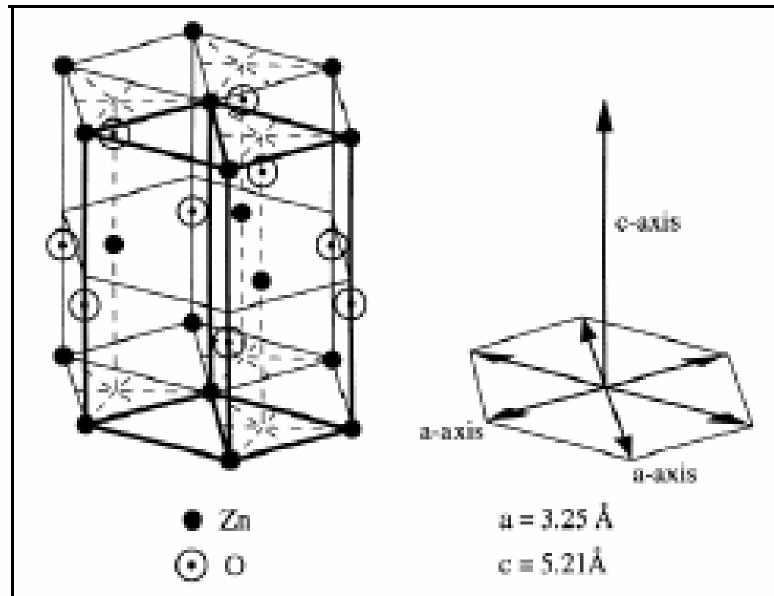

Figure 3.2 ZnO Hexagonal Wurtzite Crystal Structure [11]

3.3 Atomic Force Microscope

The AFM is typically used to detect the surface topography of a sample, and this is done by dragging a sharp tip across the samples surface, as the tip is passed over the surface it deflects vertically, giving the surface deflection along that path. By scanning many parallel paths the computers software can create a three dimensional map of the surface. This process is done on a micro to nano size scale and can give the surface roughness of a thin film on the order of a few nanometers. Since the scale is so small the tip doe not have to be in direct contact with the surface. Van der Waals forces from the surface of the film are strong enough to deflect the cantilever tip. The tip deflection is optically detected by a laser beam that is concentrated on the backside of the cantilever [25].

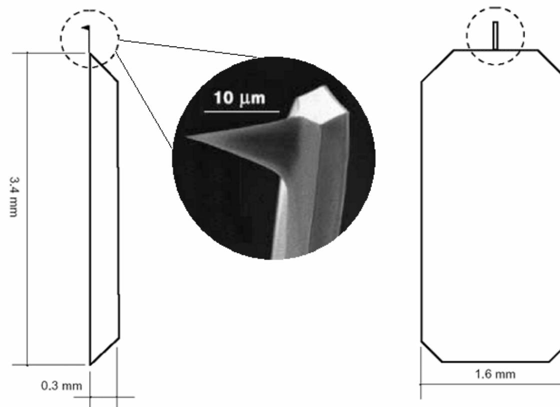

Figure 3.3 AFM Tip [26]

The AFM can also be used in detecting a thin films piezoresponse. Some AFMs are already set up for performing this type of measurement, already having the hardware

and software installed on the system. If the AFM is not already set up for this then the equipment needed to complete this measurement is a waveform generator, lock-in amplifiers, and a conductive platinum tip [27].

The basic idea of using the AFM to measure the piezoelectric response of a sample is to apply a voltage to the sample at a certain frequency, when this happens the sample will deform because of the inverse piezoelectric response. As the sample deforms the scanning tip will record the vertical displacement of the film. Knowing the applied voltage and its frequency and the height in which the film moves the piezoelectric coefficient can be calculated. The use of lock-in amplifier serves to effectively separate and remove the topography information from the actual measured piezoresponse.

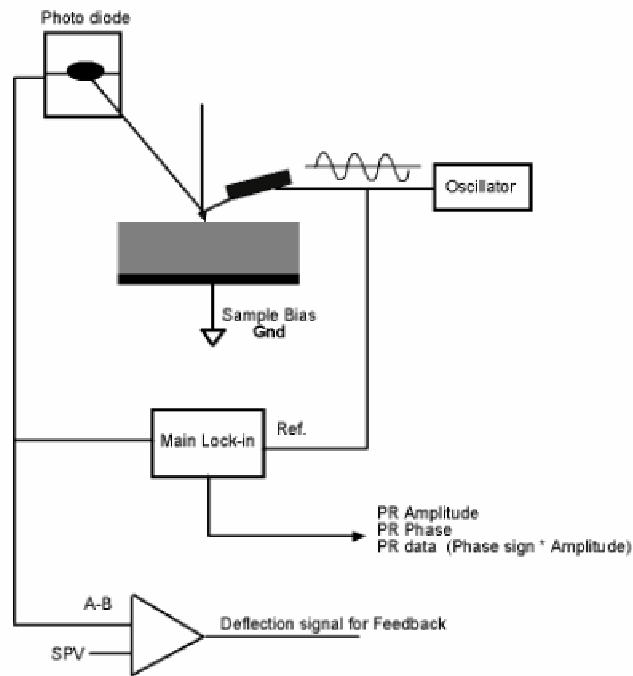

Figure 3.4 AFM Piezoresponse Schematic [28]

Before the sample can be tested for piezoresponse using the AFM, it must first be prepared properly to get the desired results. The sample must be prepared with a bottom

electrode, typically platinum, that can be probed, and the piezoelectric material is then deposited onto the electrode [28]. After the sample is prepared the instrument then operates in contact mode providing good contact between the conductive Pt tip, which acts like a top electrode, and the piezoelectric thin film [27, 29]. A waveform generator is used to supply an AC voltage to the piezo thin film [27]. When scanning the film the applied voltage is applied at a frequency too high to affect the deflection signal used in the feedback system. A frequency of 500Hz or above is adequate for this measure [30, 29]. The applied voltage makes the film resonate via the inverse piezoelectric effect. Once everything is set up, the voltage is applied, and the tip is scanning, the piezoelectric effect is measured by the use of a lock-in amplifier that receives its signal from the AFMs optical detector [27].

The primary use of this system is to study how the piezoelectric material reacts to an applied electric field [28]. One advantage to using the AFM verses another method is that it detects the properties of individual grains within the film [30]. The drawback to this technique is that it doesn't detect the bulk piezoelectric characteristics of the overall film.

3.4 Nanoindentation

Nanoindentation can be used to obtain a variety of measurements such as elastic modulus, strain hardening, fracture toughness, viscoelastic properties, and hardness. The most common measurements obtained by the system is hardness and modulus. As the

name implies the nanoindenter indents a sample on the nanometer scale or 10^{-9}m to obtain the hardness as well as the modulus of a sample.

In a conventional hardness test, a tip with a certain geometry is used to indent the sample, the residual impression is then visually inspected and measured to calculate the hardness of a material. The conventional hardness test cannot be used on thin films or silicon wafers due to the size of the films, which is why the Nanoindentation test was needed and therefore developed. The fundamental difference between the conventional method and the Nanoindentation method is that the Nanoindentation method indirectly measures the film's hardness by knowing the indenter's geometry and the depth of penetration of the indenter, versus visually measuring the indent. The average contact pressure under a fully developed plastic zone is the indentation hardness. The modulus calculation is done by taking the slope of the unloading of the load depth response [31]. An interesting point is that the two methods typically give similar results, however since the two techniques rely on different methods to determine hardness they can on an occasion have different results [31].

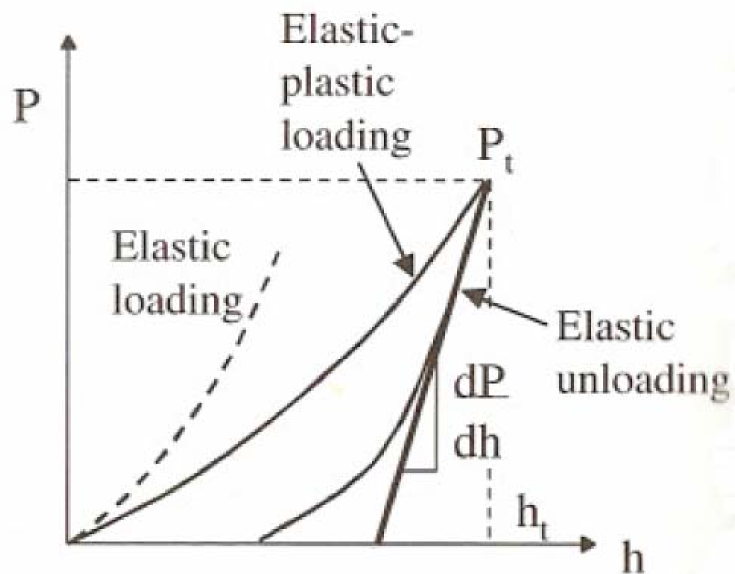

Figure 3.5 Compliance Curve [31]

Hardness is found by using the following equation:

$$H = \frac{P_{max}}{A}$$

Where *H* is the hardness, *P* is the load applied to the film, and *A* is the area.

To find the modulus we look at the slope of the unloading on the load depth response.

$$S = \frac{dp}{dh} = \frac{2}{\sqrt{\pi}} E_r \sqrt{A}$$

Where *S* is the stiffness, which is equal to *dP* over dh the change in load over the change in penetration depth. E_r is the reduced modulus, which is the combined modulus of the indenter and specimen. After the combined modulus is found we can use the following equation to find the modulus of the film.

$$\frac{1}{E_r} = \frac{(1-\nu_f^{\ 2})}{E_f} + \frac{(1-\nu_i^{\ 2})}{E_i}$$

E_f and ν_f is the modulus and the Poisson ratio of the film and E_i and ν_i is the modulus and the Poisson ratio of the indenter, which is known. Knowing the combined modulus, modulus of the indenter, Poisson ratio of the indenter, and using 0.3 for the Poisson ratio of ZnO we can find the modulus of the film.

Nanoindentation is very sensitive and has a number of things that can cause error in the results. These tests are extremely sensitive to thermal drift and mechanical vibrations. In order to isolate the instrument from any kind of vibrations, the Nanoindentation tool normally sits on top of a vibration isolator. It is also necessary to wait at least an hour after loading the sample to begin the test so that the instrument can reach thermal equilibrium. The compliance of the tip itself is another factor that needs to be taken into account in the calculation of the modulus.

Another factor that affects the measurement of the thin films is surface interactions between the tip and the film. Since the test is preformed on the nano-scale Van der Waals forces will begin to be an issue, these forces develop between molecules on the range of 100nm [31]. Surface roughness is another factor that must be taken into consideration, since the contact area is measured indirectly from the depth of indentation, a very rough sample with high asperities will give misleading information because the area of contact that is calculated will be incorrect [31]. Because surface roughness can give bad data specimens are sometimes polished. Unfortunately when a sample is polished it is put into contact with a rotating polishing wheel, this surface modification,

especially in metals, can cold work or strain harden the material [31]. As the indenter moves through the material the indenter load is not solely supported in the vertical direction, but also by compressive stresses acting inward from the sides of the film. Because the stress field is not only in the vertical direction, residual stresses, like compressive or tensile present due processing, can influence the stress field the indenter sees. A compressive stress in the film would restrict the motion of the indenter giving a higher hardness, and like wise a tensile stress would allow the indenter to move more freely through the thin film [31].

Another characteristic that influences the film's hardness is the substrate that the film is deposited on. When probing the thin film the substrate and the thin film are both compressed and act to retard the indenter's motion. That is why conventionally the max depth of penetration is typically less than 10% to minimize the influence of the substrate during the measure. Figure 3.6 shows why the indenter sees a compressive stress in the horizontal direction as well as how the substrates interaction with the thin film. Table 3.2 shows hardness and modulus values of ZnO made on various substrates.

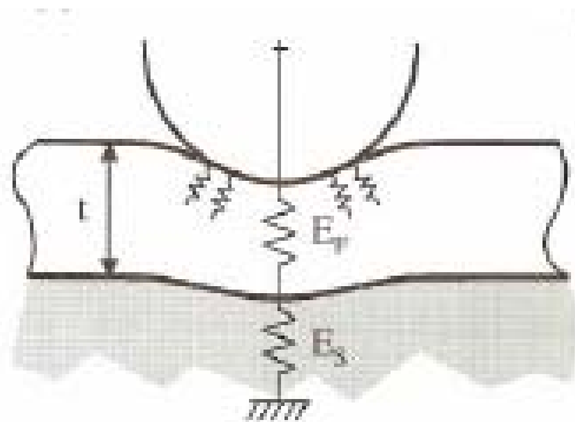

Figure 3.6 Indenter Thin Film and Substrate Interaction [31]

Table 3.2 Hardness and Modulus on Different Substrates [32]

Approximate Value	Glass	GaAs (100)	Si (111)	Si (100)
Hardness (Gpa)	8.7	9.8	10.5	9.5
Modulus (Gpa)	95	130	170	150

3.5 Film Thickness Measurements

There are several methods to obtain a thin film's thickness; two of these methods are profilometry and ellipsometry. Both methods were used in this research to obtain the thickness of various samples. The most used method was the Ellipsometer because of its ease of use, and accuracy.

The profilometer is similar to the AFM in how it works. It drags a tip or stylus across the surface of a film and records its vertical displacement across a certain path. The profilometer can run its tip over a variety of distances, varying from the nanometer range to the micrometer range giving very accurate thicknesses. The problem with using this method to determine a film's thickness at the center of a wafer is that it has to scan a longer distance, on the order of micrometers. Even though the equipment may be accurate the wafer itself is not completely flat, so when scanning that kind of distance for a thin film the profilometer will detect the film and the bend of the wafer giving an inaccurate result. Figure 3.6 shows what can happen with the warping of the substrate, as can be seen the thickness at the edge may not be the same as that in the middle. So, in order to get around this problem the sample must be masked at the center of the wafer to give a good step point where the tip can scan from a bare piece of silicon to the highest

point over a short distance so that the bending of the wafer, if any, is negligible over the short distance. This is why the Ellipsometer was used in most of the measurements instead of the profilometer, it doesn't require masking or a bare point of silicon to get a base point. It does on the other hand need an estimate height of the film in order to give an accurate result; this estimate came from the profilometer results.

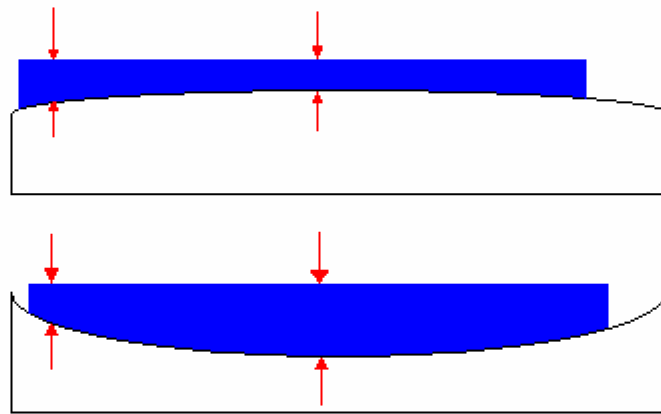

Figure 3.7 Illustration of Warping of a Substrate

Ellipsometry works by detecting the change in polarization of light reflected off of the surface of the sample. This kind of measuring technique has to use a monochromatic light source to obtain a time-invariant phase relationship between two waves; this is why a laser is used as the light source [33]. The light that passes through the film and reflects off of the substrate undergoes a phase change due to its path length and interface with the material. The light that is reflected off of the sample has its amplitude ratio and phase relationship of E_p and E_s measured. This information is used to determine the ellipsometric angle Ψ and Δ [33]. The mathematics of converting the raw data collected into Ψ and Δ and then into a thickness measure is done by the instruments software [33].

Ellipsometry is very accurate and very reliable, able to calculate a film's thickness on the order of angstroms. The only draw back to this kind of measurement is that it is an indirect method relying on a phase change to determine thickness. A thin film grown can give off the same phase change at various thicknesses, just like the color of the film changes and then repeats itself as a film is grown. Because this phase change will eventually repeat itself, an initial guess of how thick the film is must be made. The software uses this guess to give the thickness of the film in that range. In order to use this technique accurately a basic understanding of the film being deposited must be know to get the initial guess. That is why profilometry was first done on a few samples before using the ellipsometer. The use of the profilometer gave a basic understanding of ZnO deposition rates.

3.6 Normal Load Method

In order to find the piezoelectric properties of a film two different techniques can be used, using the direct piezoelectric effect and the inverse piezoelectric effect. Finding the piezoelectric coefficient through the direct method involves straining the film and measuring the voltage obtained from a given amount of strain. The inverse method involves applying a voltage to a film of structure to and measuring the amount of strain obtained for the amount of voltage applied. The Normal Load method uses the direct piezoelectric effect to calculate the piezoelectric coefficient.

The ZnO film was deposited onto a metal substrate; the metal substrate acts like a bottom electrode. A load is then applied to a metal tip, which acts like the top electrode.

When the load is applied the piezoelectric layer produces a charge, which can be measured by a multimeter. By knowing the load applied and measuring the voltage the piezoelectric coefficient can be calculated. We can use the following equation to do so.

$$d_{33}=Q/F=C_m V_m /F$$

The piezoelectric coefficient d_{33} is equal to the Charge Q divided by force F. To find the charge we can put a capacitor in parallel in the circuit, since capacitance equals the charge over the voltage we get the charge by multiplying the voltage measured by the capacitor used.

Figure 3.7 shows the schematic of the system as was used by K. Lefki and G.J.M Dormans in “Measurement of Piezoelectric Coefficient of Ferroelectric Thin Films”.

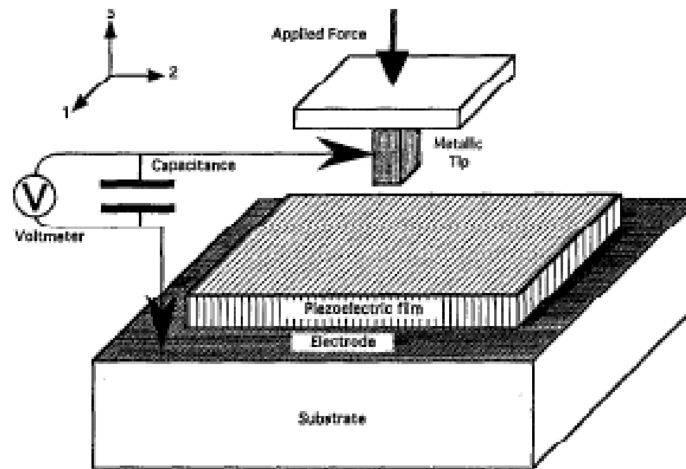

Figure 3.8 Schematic of Normal Load Method [34]

3.7 FTIR

Fourier Transform Infrared Spectroscopy (FTIR), much like the XRD, is a useful tool in identifying a material. This technique measures the infrared intensity that passes through the substance compared to wavelength. The IR light that passes through the material interacts with the materials atomic bonds at a specific wavelength. As the light interacts with the bonds it causes then to stretch and vibrate, this interaction is what absorbs the IR light. The frequencies of vibration are determined by the molecules shape, and mass of the atoms bonded. This is why different materials interact differently with the IR light, when the IR absorption spectrum is analyzed it can show what kind of material is being looked at. The absorbance of the material is proportional to its concentration.

This method measures all wavelengths simultaneously by guiding the light through an interferometer. By performing the Fourier transform on the data, the results get mathematically adjusted to be identical to those of a conventional infrared spectroscopy. FTIR instruments are cheaper and faster to use than the conventional spectrometers.

CHAPTER FOUR: RESULTS AND DISCUSSION

4.1 Optimization of Pulse Laser Deposition (PLD)

Many films were made by PLD method and then characterized by AFM, XRD, and Nanoindentation. The experiments were carried out by using a KrF excimer laser (Lambda Physics Inc., LPX 210i). The laser light had a wavelength of 248nm, with the energy set at 200mJ, a repetition rate of 10Hz, and the target was spaced 40mm away from the substrate. The substrate temperature and oxygen pressure where the only variables adjusted throughout the research. The typical deposition time for the films was twenty minutes, the only exception to this was the film characterized by the nanoindenter, which had a deposition time of a 100 minutes to get a film thickness on the order of a micron.

The typical experimental procedure was to first clean a silicon (100) substrate with acetone and methanol to remove any contaminants off of the surface. The sample was then loaded onto the substrate holder, put into a stainless steel vacuum chamber, and then sealed inside. A roughing pump was then used to bring down the chamber pressure from atmospheric to approximately 50 millitorr of pressure, at that point a turbomolecular pump was operated to further bring down the pressure to 10^{-6} torr. Once the desired pressure was reached the substrate temperature was adjusted and oxygen was introduced.

The laser and target rotator was turned on and the deposition took place for. The target that was used was a pure ZnO target. The laser was operated in 10-minute intervals with a 5-minute break in between operations to prevent the laser from overheating since it does not have a cooling system. After the deposition was completed the laser was turned off and the substrate was allowed to cool to a temperature below 50˚C before the chamber was vented and the sample was taken out.

Table 4.1 Experimental Conditions for the PLD

Date	Experiment #	Temp (C)	Pressure (mT)	Time (min)	Substrate
3/30/07	1	300	200	20	Si
4/3/07	2	300	Vacuum	20	Si
4/9/07	3	300	200	20	Glass
5/4/07	4	400	200	20	Si
5/17/07	5	200	200	20	Si
6/15/07	6	22	200	20	Si
6/18/07	7	100	200	20	Si
6/21/07	8	22	200	20	Si
6/21/07	9	200	100	20	Si
6/25/07	10	200	50	20	Si
6/28/07	11	200	100	100	Si
7/2/07	12	50	100	20	Si
7/3/07	13	75	100	20	Si
7/10/07	14	200	100	20	Glass
7/14/07	15	75	100	20	Si
7/17/07	16	22	100	20	Si
7/17/07	17	100	100	20	Si
7/19/07	18	75	200	20	Si

4.1.1 Substrate Temperature Effects

Heating the substrate gives energy for the formation of a crystal orientation in the film being deposited [14]. Therefore adding energy to the system is crucial in depositing a thin film of good crystal orientation. This being the case, someone might think the more energy the better, unfortunately this does not hold true, if too much energy is added to the system when the film is deposited some problems can occur. Since the substrate and the ZnO being deposited are two different materials, they of course have different thermal expansion characteristics. So if a substrate is heated to a high temperature in the deposition things might be fine, but when the sample is cooled to room temperature residual stresses can form. Too much energy can create stresses and if there is not enough energy the film will not crystallize properly, a happy median has to be found.

The initial two experiments where preformed at 300˚C at $2.2*10^{-5}$ torr with no oxygen pressure and also at an oxygen partial pressure of 200 millitorr. This initial experiment was done to see if a partial pressure of oxygen does in fact help in the growth of thin films. As seen in Figure 4.1 the peak intensity, position, and shape is better with the sample that had the partial pressure of O_2 in it. The peak position of ZnO with the (002) orientation is supposed to be at 34.442˚, the sample done at 200 millitorr is close to this value.

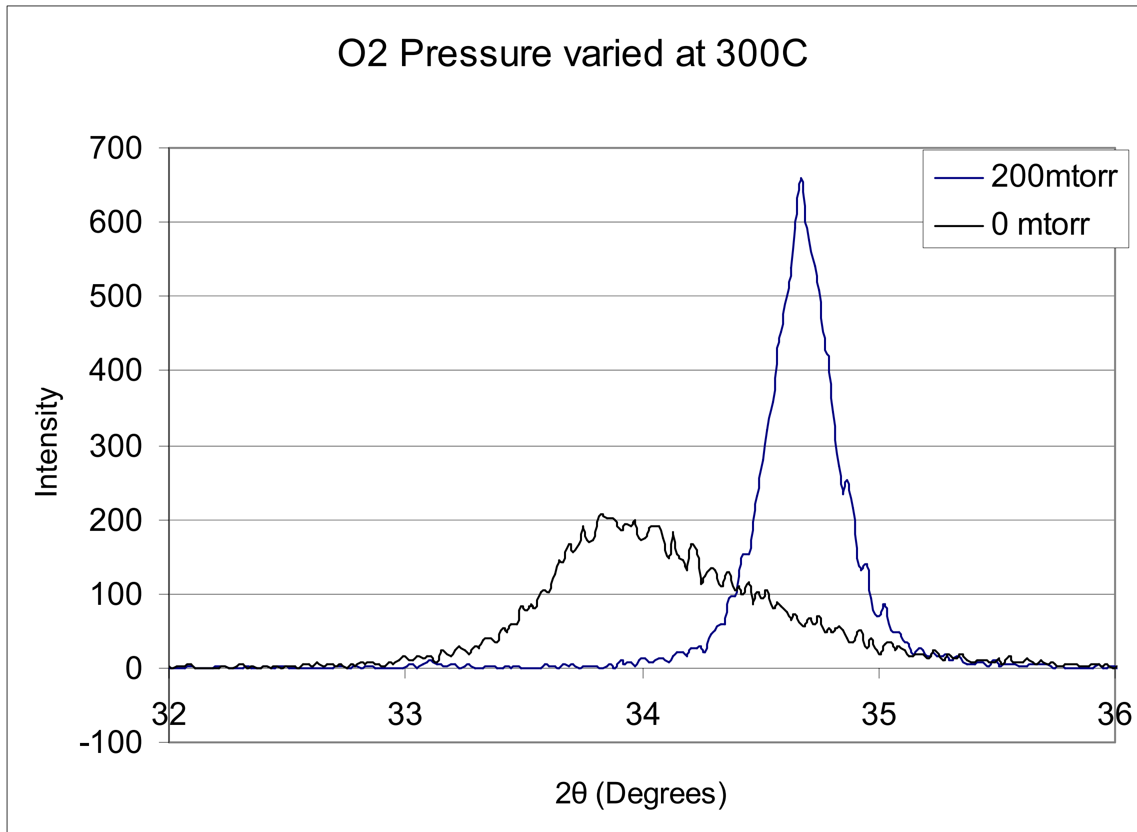

Figure 4.1 O_2 Pressure Varied at 300°C

So, yes it does help, and at this point the temperature was varied from room temperature to 400˚C at 200 millitorr. Figure 4.2 shows the XRD results of samples done at various temperatures. The peak intensity is shown to increase with increasing temperature, going from an amorphous film at room temperature to having a very high peak intensity at 400˚C. The peak position also changes with increasing temperature going from 34.30˚ to 34.71˚. The XRD results were further characterized by Bragg's Law to find the interplanar spacing and Scherrer's equation to find the crystallite thickness of the samples. Scherrer's equation gives us two things, of course the crystallite thickness, and also since the equations uses the full width at half max (FWHM) value in the calculation, a bigger crystallite size corresponds to a smaller FWHM and, therefore, a

bigger crystallite thickness is more desirable. Keeping in mind that the end result is to use ZnO in a cantilever resonator a film with no residual stresses is desired, along with a good crystallite thickness, which will give the best piezoelectric effect. Even though the film grown at 400˚C has the best peak intensity and best crystallite thickness, it also has some tensile stress in the system, which can be seen from its peak position and calculated interplanar spacing.

Table 4.1 shows the values obtained from the XRD results in that table the stress of the film was calculated by first finding the strain in the film by the following equation. ε is the strain, Δd is the interplanar spacing of unstrained ZnO minus the interplanar spacing found experimentally, where d_o is the unstrained interplanar spacing.

$$\varepsilon=\Delta d/d_o$$

Knowing the strain we can then calculate the stress σ by the following equation found in “Thin-Film Deposition Principles and Practice” by Donald L. Smith.

$$\sigma_{x,y}= \varepsilon_{x,y} E/(1-v)$$

E is Young’s modulus of ZnO as found from the nanoindenter measurements, ε is found from the above equation and the Poisson ratio v is 0.3. In Table 4.2 a positive stress shows that the film is in tension and a negative stress shows that the film is in compression.

The film grown at 200˚C with its peak position at 34.59 is the film that has the closest value to the desired 34.442˚ along with a good crystallite thickness and peak intensity. The crystallite thickness of this film is very close to the other films grown at higher temperatures. Figure 4.2 shows the various XRD results at the different temperatures. Even though the lower temperature films have less residual stress, they also

have smaller crystallite thickness than the 200˚C sample, as well as having a very low peak intensities. So, taking all things into consideration the peak intensity, peak position, and the crystallite thickness, the best sample was the one deposited at 200˚C at the given pressure. At this point the oxygen pressure was altered in order to optimize the mean free path of the system for the best deposition rate.

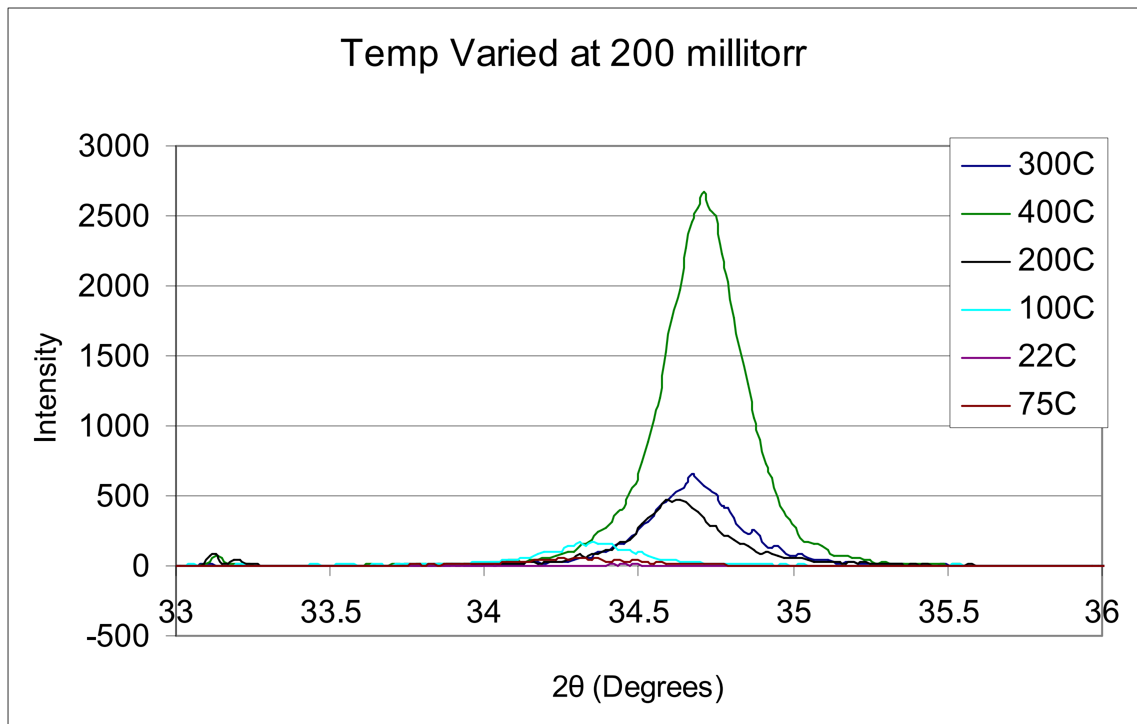

Figure 4.2 Temperature Varied at 200 Millitorr

Table 4.2 XRD Analysis Based on Temperature Variations at 200 Millitorr

Temperature (˚C)	d_{002} (Å)	Crystallite thickness (nm)	2θ	σ (GPa)
22	NA	NA	NA	NA
75	2.61183	21.64	34.30	-0.84058
100	2.61183	25.7	34.31	-0.84058
200	2.59132	29.4	34.56	1.1853
300	2.58553	29.4	34.67	1.7572
400	2.582639	30.5	34.71	2.0428
ZnO Reference	2.60332	NA	34.422	NA

4.1.2 O_2 Partial Pressure

The initial step in the experimentation was to determine if oxygen was needed in the system to help in the formation of ZnO, the second step was to optimize the temperature, now the amount of O_2 needed in the system will be analyzed to optimize the men free path and still have excellent formation of ZnO. Like the substrate temperature, this will be a balancing act, having too much oxygen will reduce the mean free path and having not enough will effect the formation of the ZnO, leading to excess zinc in the film. Since it was concluded from the previous set of experiments that the best temperature

was at 200˚C, the pressure experiments were preformed at 200˚C, at the following pressures 50, 100, and 200 millitorr.

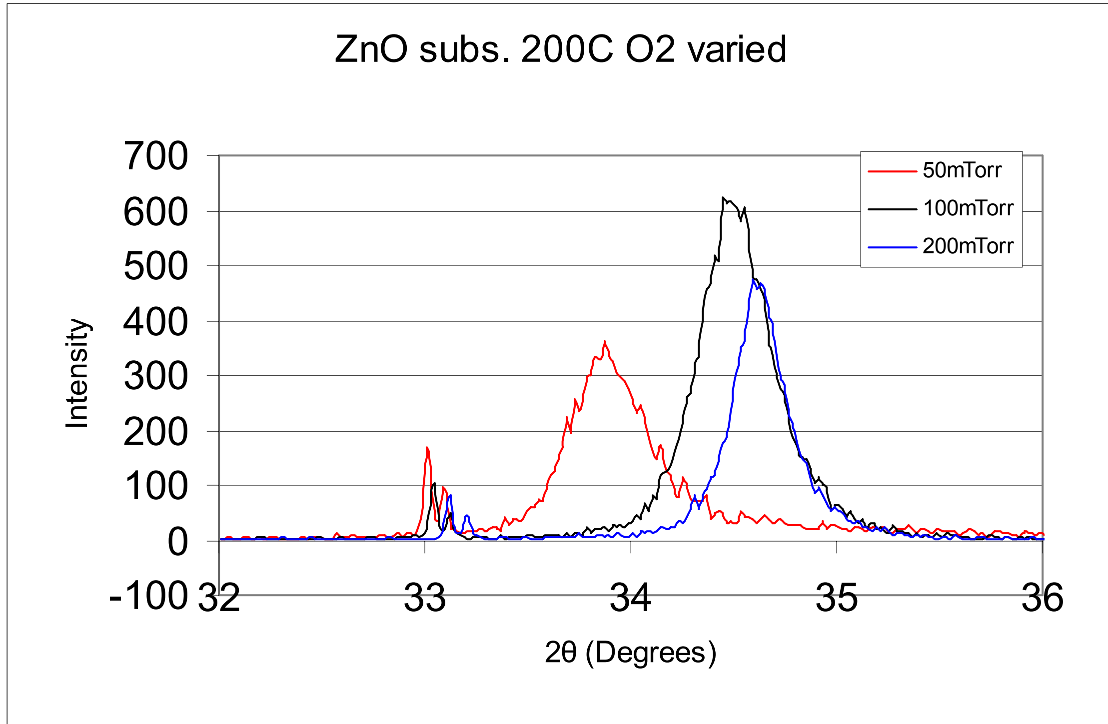

Figure 4.3 ZnO Grown at 200˚C at Various Pressures

Based on the results shown in Figure 4.3 the optimum pressure is at 100 millitorr, it has the best peak intensity, position, and good crystallite thickness. The peak position is 34.45˚, showing that there is almost no residual stress in the film. Table 4.3 shows the calculated interplanar spacing of the samples along with the crystallite thickness and residual stress in the film. From the table you can see that the partial pressure of oxygen has an effect on the residual stress in the films, going from a compressive stress at lower pressures to a tensile stress at higher pressures.

Table 4.3 XRD Analysis Based on Pressure Variations at 200˚C

Pressure (millitorr)	d_{002} (Å)	Crystallite thickness (nm)	2θ	σ (GPa)
ZnO Reference	2.60332	NA	34.422	NA
50	2.64475	21.61	33.87	-4.08225
100	2.59861	21.65	34.45	0.46523
200	2.59132	29.40	34.56	1.1853

4.1.3 Temperature Variations at 100 Millitorr

Even though the temperature was previously varied at 200 millitorr, the samples were remade at 100 millitorr at various temperatures to see the effects of temperature at the optimum pressure. The temperature was varied from room temperature to 200˚C, making the films at these low temperatures was partly done to see if we could get a mono-crystalline structure that could feasibly be grown on a polymer. The growth of thin films on polymers is beyond the scope of this research; however a few experiments were conducted to see if it is feasible to do. Growing a crystalline thin film at low temperatures could lead to other applications in the future.

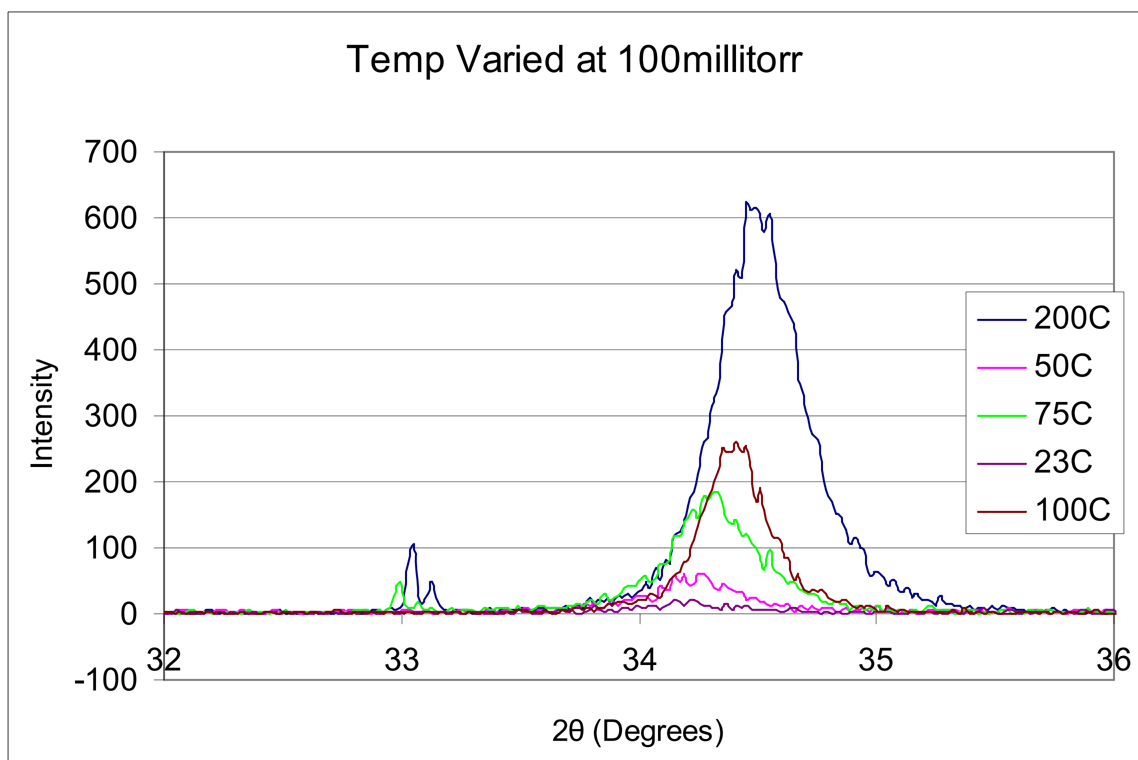

Figure 4.4 Temperature Varied at 100 Millitorr

Table 4.4 XRD Analysis Based on Temperature Variations at 100 Millitorr

Temperature (˚C)	d_{002} (Å)	Crystallite thickness (nm)	2θ	σ (Gpa)
22	NA	NA	NA	NA
50	2.617749	25.69	34.25	-1.42522
75	2.6103524	21.64	34.33	-0.69463
100	2.604466	27.42	34.41	-0.1132
200	2.59861	21.65	34.45	0.46523
ZnO Reference	2.60332	NA	34.422	NA

From this data the 100˚C has the best interplanar spacing and peak position out of all the samples, however when compared to the 200˚C sample it doesn't have the best peak intensity. Even though the 200˚C sample doesn't have the values as close to those found by the 100˚C sample, they are very close, and what can be seen later is that the deposition rate and roughness are better for the 200˚C sample versus the 100˚C sample.

4.1.4 FTIR

The infrared light was irradiated perpendicularly to the film's surface. Since the ZnO showed a c-axis orientation growth the infrared light that interacted with the film was perpendicular to the c-axis of the film. The frequency of an optical phonon is split into longitudinal optical (LO) and transverse optical (TO) components. Figure 4.5 shows the FTIR results of two samples grown at 100 millitorr. The peaks were observed at 407cm^{-1} for the 200°C sample and 402cm^{-1} for the 75°C sample, corresponding to the E_1 (TO) mode for ZnO. Zinc oxide's E_1 (TO) mode occurs at 412cm^{-1}. The difference in frequency could be associated with the slight differences with the interplanar spacing of the two samples. The higher temperature sample has a higher absorbance indicating good concentration, and this could be due to the fact that the higher temperature sample has a higher deposition rate, and therefore more ZnO molecules to interact with the IR light. Both results shows that the IR light was absorbed at the appropriate value for ZnO indicating that the IR light did in fact interact with the ZnO bonds proving that the zinc and the oxygen combined correctly to form ZnO.

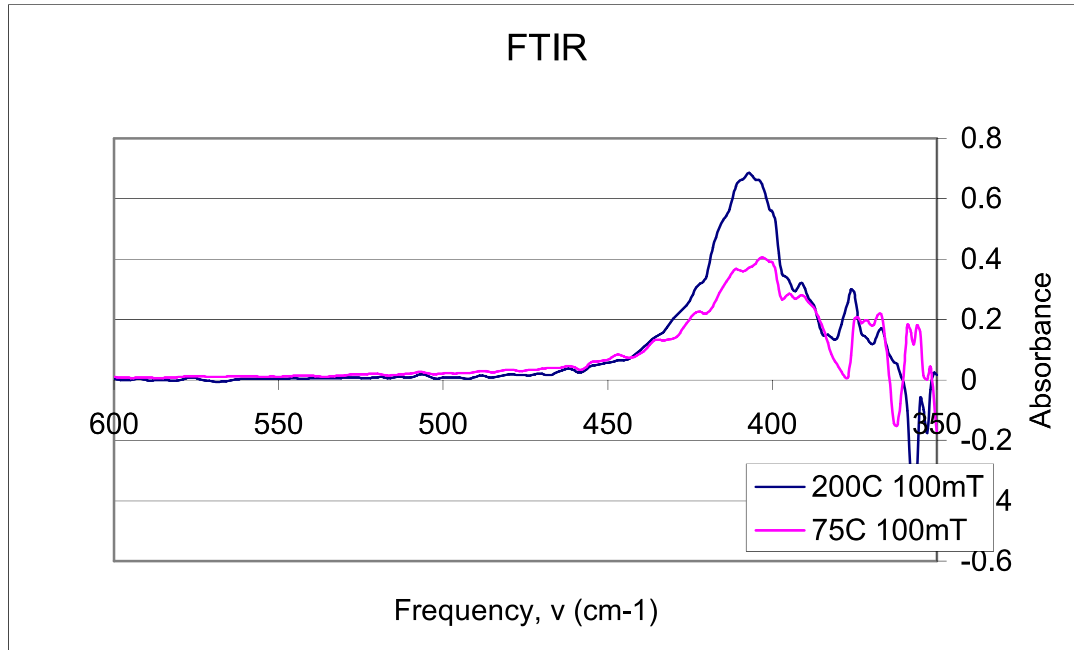

Figure 4.5 FTIR Results

4.1.5 Surface Roughness

The surface roughness was characterized by the AFM, the AFM calculated the surface roughness of the samples in nanometers as well as giving us a visual 2D and 3D view of the samples topography. Figure 4.6 graphically shows the roughness of all the thin films made by the PLD. For making a thin filmed device, a high surface roughness value could create a problem. Large asperities could locally interfere with the piezoelectric effect or the bonding of other material onto the surface of the ZnO. The surface roughness of the film grown at 200˚C with a pressure of 100 millitorr has roughness of 3.6nm, which is a very reasonable result. The lower temperature results

have somewhat odd values having a very low surface roughness at room temperature, the samples then increase in roughness as they reach 75ºC or 100ºC and then the roughness drastically decreases. Since this seems odd, several extra samples were made at the 75ºC temperature and analyzed to see if it was accurate. All of the results from the samples made at this temperature came out to be very similar. For the films grown from 200-400ºC the roughness increased slightly just like the crystallite thickness of the films did.

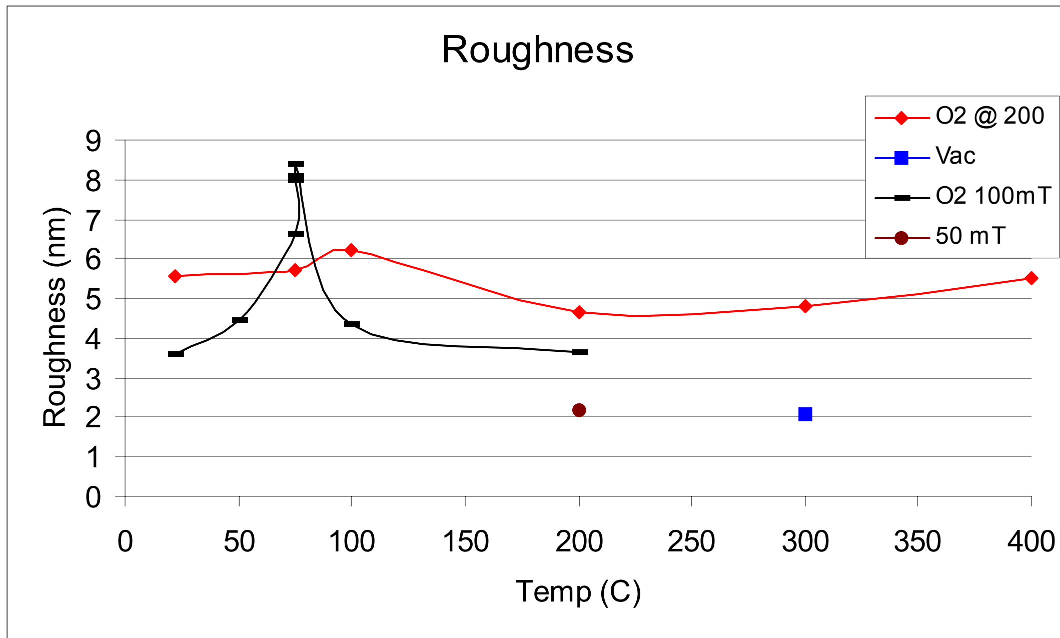

Figure 4.6 PLD Surface Roughness

The next few figures are the AFM images received from the best film. One shows a three dimensional image of the surface topography of the sample and the other image shows the surface roughness measure of the sample.

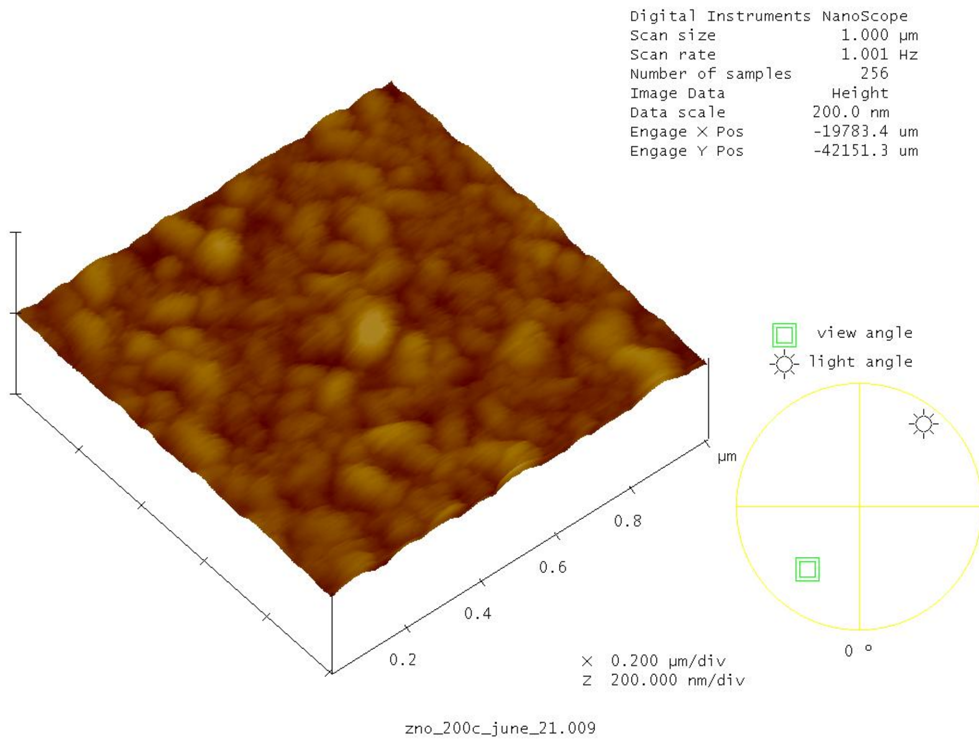

Figure 4.7 3-D View of the Surface Topography

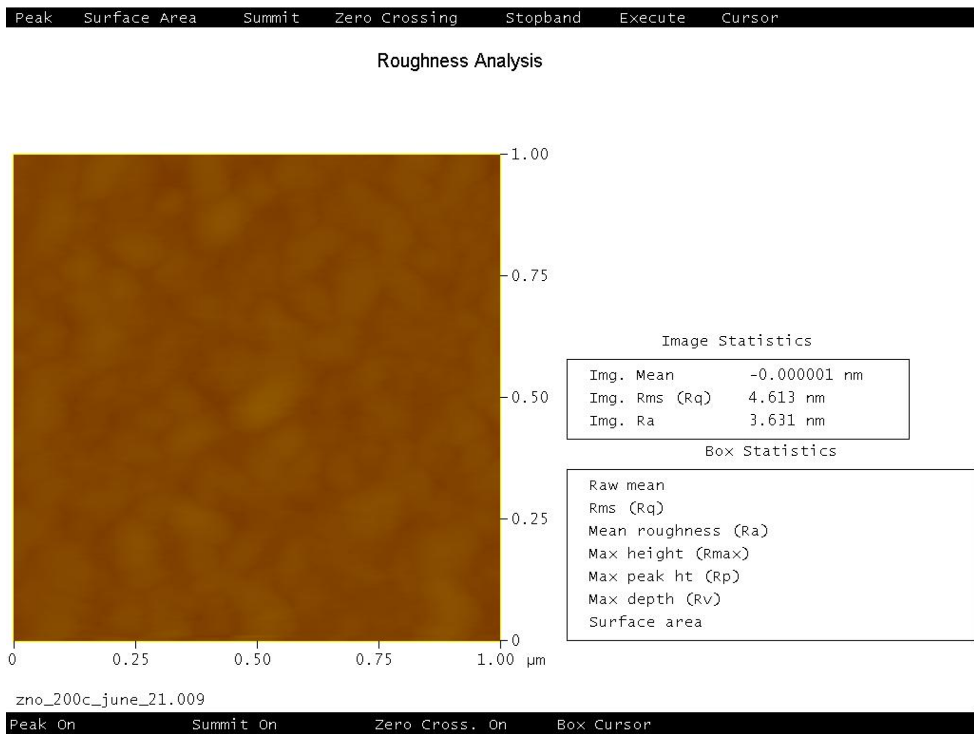

Figure 4.8 Surface Roughness

4.1.6 Deposition Rates

Ellipsometry measurements were preformed to obtain the deposition rates of the films grown at various pressures and temperatures. Not all of the samples were measured but a few conclusions can be formed based on the results that were obtained. What can be seen from the results is that if the pressure is held constant at various temperatures the deposition rate increases with increasing temperature. It stands to reason that with more thermal energy in the system it is easier for the film to form into its crystal structure.

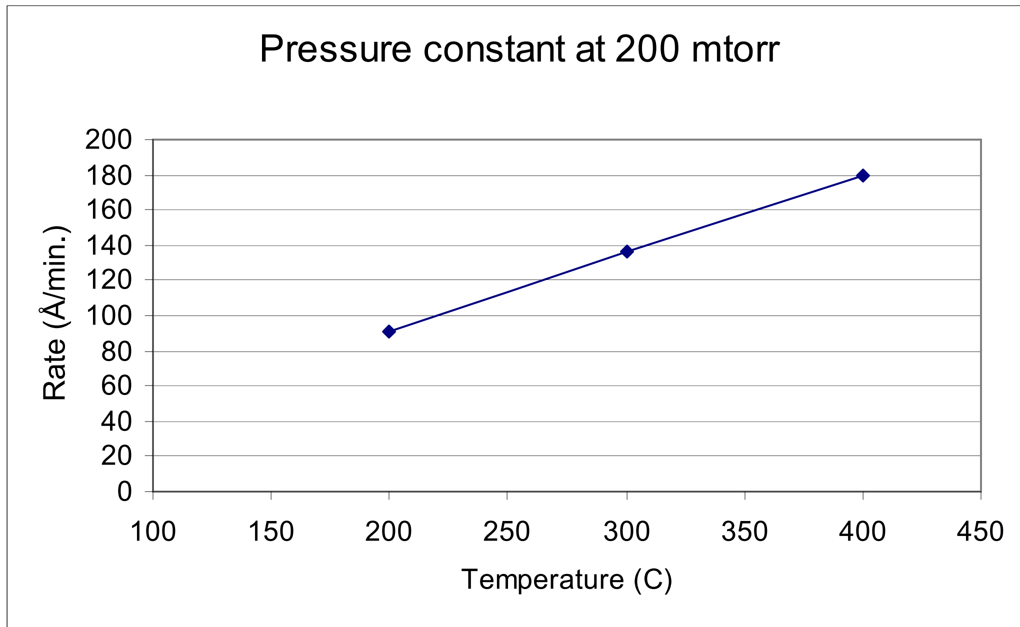

Figure 4.9 Deposition Rate at Various Temperatures

What can also be seen from the ellipsometer data is that when pressure is varied at a select temperature the deposition rate increases with decreasing pressure. This of course confirms that a reduction of pressure increases the mean free path making it easier for the ions to travel the distance from the target to the substrate.

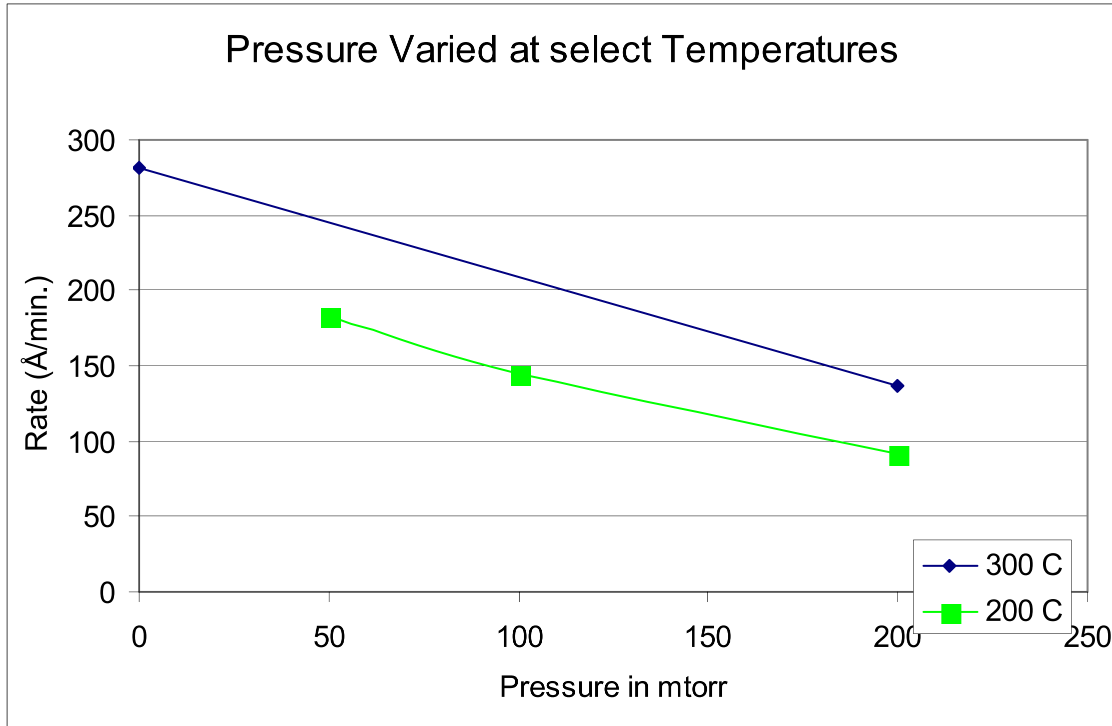

Figure 4.10 Deposition Rate at Various Pressures

4.1.7 Nanoindentation

Nanoindentation was used to measure the film's modulus and hardness. The film that was grown to obtain these measurements was grown for 100 minutes to obtain a thickness of at least a micron, from the calculated deposition rate of the sample deposited at 200ºC with a pressure of 100 millitorr the film thickness should be approximately 1.5 microns. The nanoindenter indented the sample to a depth of 1700nm to acquire information over a decent depth. Sixteen indentations were preformed at different locations on the film to obtain an average of both the hardness and modulus.

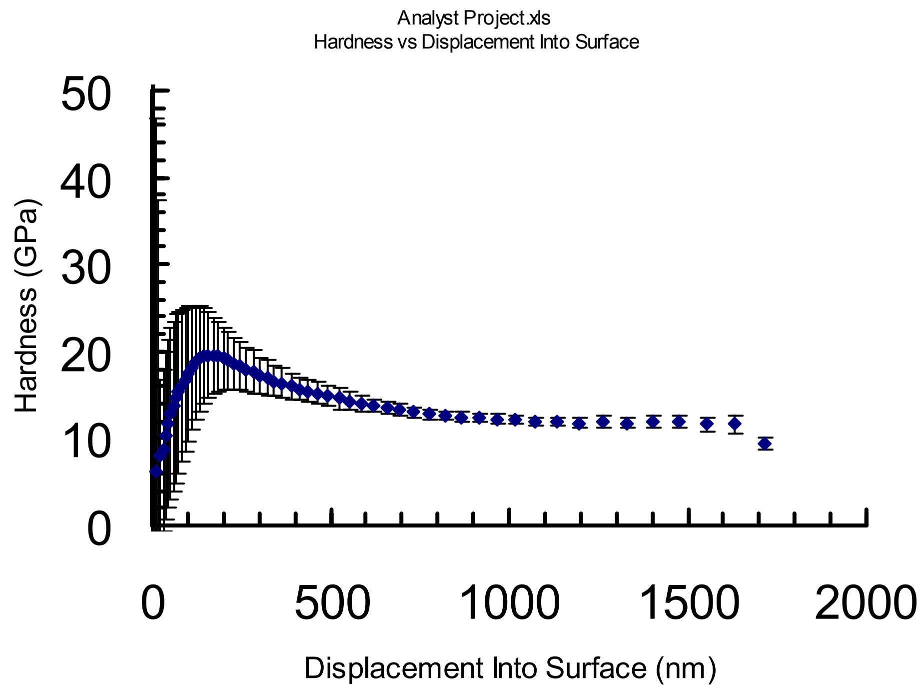

Figure 4.11 Hardness

The thin film's hardness plateaus at around 500nm to 1500nm, showing very little error in this range. A hardness of 12GPa was found. This value is close to Han-Ki Yoon and Yun-Sik Yu's findings of 9.5-10.5GPa . Even though the depth of penetration to obtain a good value was greater than the conventional 10%, according to "Nanoindentation" by Anthony C. Fischer-Cripps "research suggests that this rule has no physical basis". It appears the substrate had very little effect on the hardness measure seeing that the measured values reached the value of 12GPa and stabilized at that value until the depth of penetration reached 1700nm. At 1700nm the value suddenly changes, this is probably because the film is only about 1700nm thick and the indenter has reached the point where the zinc oxide meets the silicon.

The modulus of the thin film was also measured by the Nanoindentation technique. It's similar to that of the hardness verse indentation depth graph, in that it has a high value at low indentation depths and then line plateau at a value of 500-1700nm, with a modulus of 180GPa. The high values at the initial penetration could be due to the film's surface roughness and Van der Waals forces interacting with the indenter. At the higher penetration depths we were able to get more accurate values for the modulus. However the value of 180GPa is higher than the values achieved by Han-Ki Yoon and Yun-Sik Yu's, whose value for modulus ranged from 150-170Gpa for ZnO deposited onto silicon. Both the hardness and the modulus have very little error in the results, giving values on the same order of magnitude as those achieved by Han-Ki Yoon and Yun-Sik Yu.

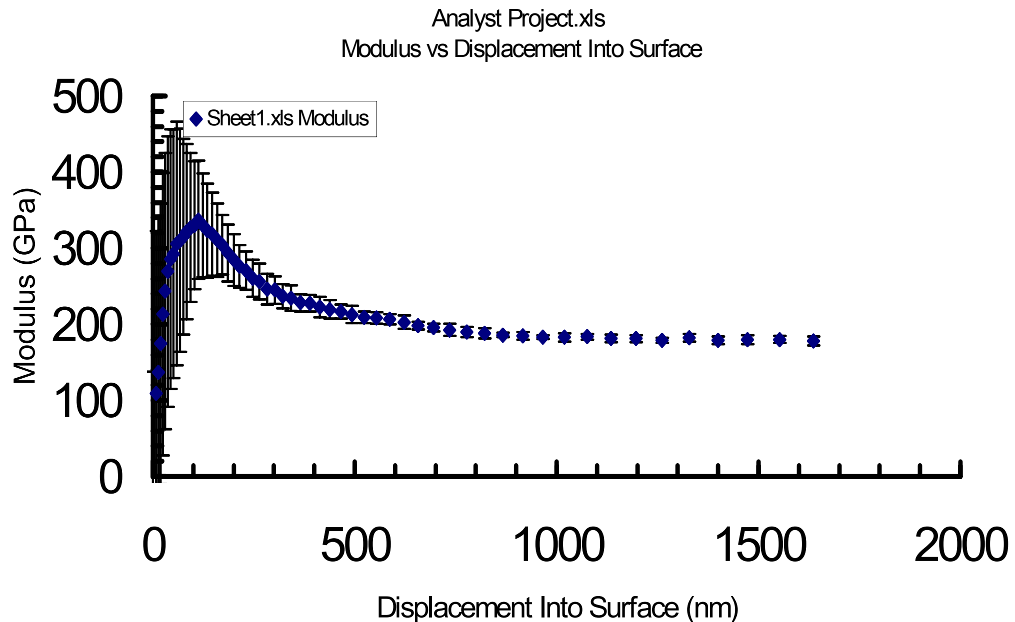

Figure 4.12 Modulus

4.1.8 Conclusion for the Optimization of PLD

Many films were made at various deposition conditions to find the optimum "recipe" to grow a thin film. Other films may show better qualities when analyzed by any one instrument, however, when taking all things into consideration the optimum condition was at a substrate temperature of 200°C at 100 millitorr. This film showed the best combined XRD and AFM results, along with the best deposition rate.

4.2 Optimization of Sputtering Depositions

After characterization of the thin films was performed with the PLD system, films were then deposited by Sputtering. The Kurt J. Lesker Company CMS-18 Thin Film Deposition System was the equipment used in these experiments. The films obtained through the sputtering technique were characterized by AFM, XRD, profilometry, and ellipsometry. The variables that were adjusted to obtain an optimum film were the RF power, substrate temperature, and the argon to oxygen flow rate into the chamber. The pressure in the system was kept at approximately 16 millitorr for every deposition, with a typical deposition time of 5 hours. A pure ZnO target was used in the depositions, and this target was 80mm away from the substrate. The substrate holder rotated in every deposition to help the film grow uniformly.

The typical experimental procedure was to first clean a silicon (100) substrate with acetone and methanol to remove any contaminants off of the surface. The sample

was then loaded onto the substrate holder and put into the stainless steel vacuum chamber. The chamber was then wiped down with methanol to remove any excess particulates before the chamber was sealed. A roughing pump was operated to decrease the chamber pressure from atmospheric pressure to approximately 50 millitorr, at that point the cryo-pump was used to bring the pressure down to $2*10^{-6}$ torr. At that point, argon and oxygen was pumped into the chamber at a specified flow rate to get a chamber pressure of 16 millitorr. The flow rate is in SCCM (standard cubic centimeter per minute) and the argon to oxygen ratios were done in percent flow rate. After the flow was set to get the desired pressure the RF power was increased to 60 watts, at which point the shutter over the target was opened temporarily to allow the matching network to tune to the ZnO target. Once the matching network tuned to the target, plasma formed in the chamber, and the shutter was then re-closed. The power was increased until it got to the desired value. Once the power was set, the substrate temperature was adjusted and the deposition took place. After the deposition was done the RF power was reduced, along with the temperature, and the gasses were shut off. The substrate was allowed to cool down to about 50˚C before the chamber was vented and the sample was taken out.

Table 4.5 Experimental Conditions for Sputtering

Date	Exp. #	Power (W)	Ar:O_2	Temp (C)	Time (hrs)	Substrate
7/26/07	1	100	100:0	200	2	Si
7/26/07	2	125	100:0	200	2	Si
8/1/07	3	100	75:25	200	5	Si
8/2/07	4	150	75:25	200	5	Si
8/3/07	5	200	75:25	200	5	Si
8/7/07	6	250	75:25	200	5	Si
8/9/07	7	100	100:0	200	5	Si
8/13/07	8	100	60:40	200	5	Si
8/14/07	9	250	75:25	400	5	Si
8/16/07	10	250	75:25	300	5	Si
8/21/07	11	250	75:25	200	2.5	Si
8/21/07	12	100	75:25	200	2.5	Si
8/23/07	13	250	75:25	300	5	Si
9/12/07	14	250	75:25	400	3.88	Si/SiO_2/Pt
						Metal
9/18/07	15	250	75:25	200	4.15	Si/SiO_2/Pt
						Metal
9/25/07	16	250	75:25	300	4.78	Si/SiO_2/Pt
						Metal

4.2.1 Argon to Oxygen Flow Rate Ratios

Much like in the PLD experiments, we knew that oxygen would be needed in the chamber to help in the formation of zinc oxide; the question was how much oxygen. Having too much oxygen will reduce the amount of argon in the chamber as a result reducing the amount of ions used to sputter off the target material. Likewise, not enough oxygen in the chamber and excess zinc might form on the substrate. So the initial depositions were done at a chamber pressure of 16 millitorr. The substrate temperature

was set to 200°C, since that is what was favorable in the PLD experiments, and a relatively low RF power of 100 watts was used. Three experiments were performed at various argon to oxygen flow rates, one at 100% argon in the chamber, another one had a flow rate of 75% argon to 25% oxygen, and the last deposition had 60% argon to 40% oxygen. Figure 4.14 and Table 4.6 show the results of the depositions.

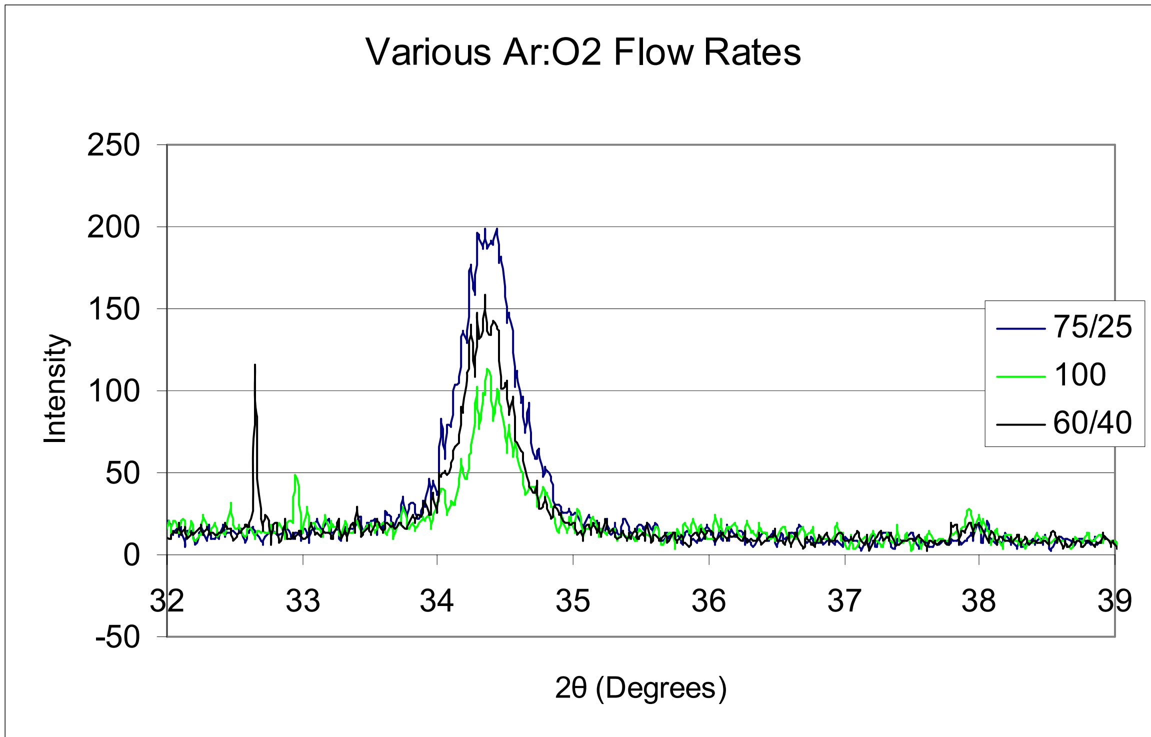

Figure 4.13 Various Ar:O_2 Flow Rates

Table 4.6 XRD Analysis Based on Various $Ar:O_2$ Flow Rates

$Ar:O_2$ Flow Rates	d_{002} (Å)	Crystallite thickness (nm)	2θ	σ (GPa)
ZnO Reference	2.60332	NA	34.422	NA
100	2.604466	22.226	34.39	-0.1132
75/25	2.602999	17.50	34.43	0.031707
60/40	2.608878	22.23	34.35	-0.54899

Based on Figure 4.14 and Table 4.6 it was concluded that the best film was the one grown in a 75:25 percent flow rate of argon to oxygen. At this flow rate there was the least residual stress in the film and it had the best peak intensity over the other two samples. Unfortunately, the crystallite thickness was not as high as the other two films. However, it was still on the same order of magnitude. The 75:25 condition was the optimum argon to oxygen flow rate, and was used in the rest of the experiments.

4.2.2 RF Power

After the $Ar:O_2$ flow rate was determined films were then grown at various RF powers, starting at 100 watts and increasing by increments of 50 watts up to 250 watts. This was done to increase the deposition rate of the ZnO onto the substrate. At 100 watts of power the sample would only grow about 80nm in 5 hours. Power was the only thing varied in this set of experiments so the $Ar:O_2$ flow rate was 75:25, chamber pressure was

kept at 16 millitorr, substrate was heated to 200°C, and the films were deposited for 5 hours.

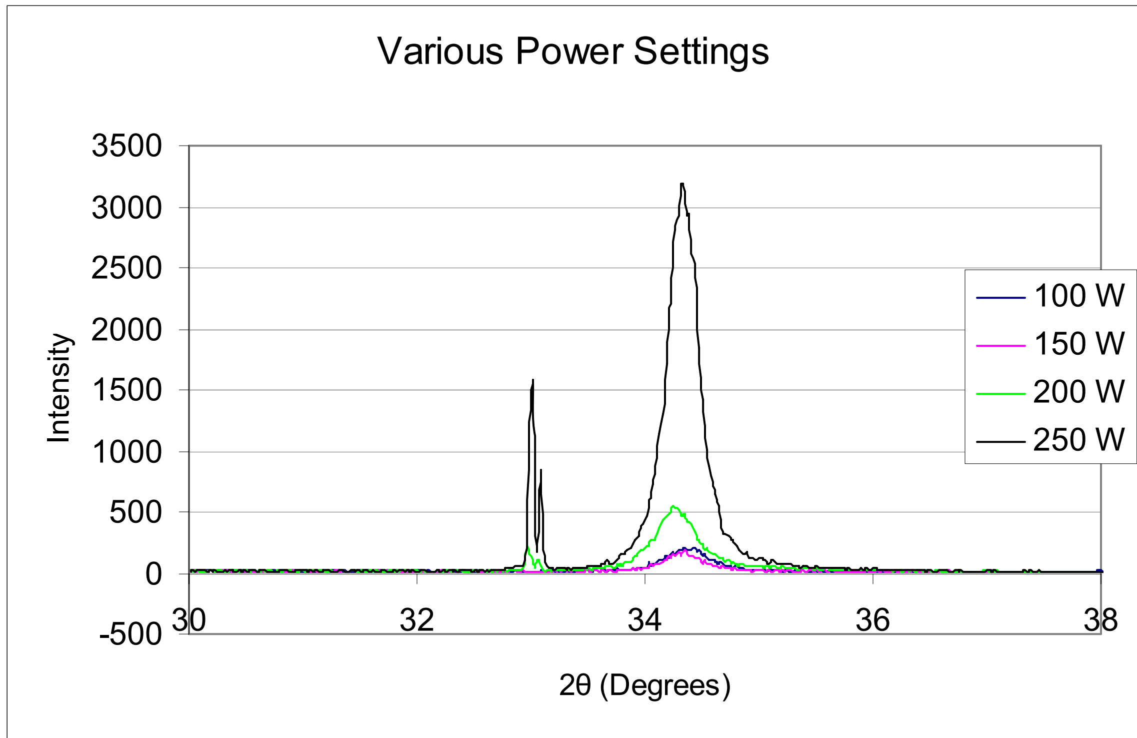

Figure 4.14 Various Power Settings

Table 4.7 XRD Analysis Based on Various RF Power Settings

Power (W)	d_{002} (Å)	Crystallite thickness (nm)	2θ	σ (GPa)
ZnO Reference	2.60332	NA	34.422	NA
100	2.602999	17.50	34.43	0.031707
150	2.608878	24.19	34.37	-0.54899
200	2.616266	21.63	34.29	-1.27874
250	2.611828	26.52	34.31	-0.84038

Based on Table 4.7 the film that has the best interplanar spacing and therefore the least amount of residual stress in the film is the film made at 100 watts of power. Unfortunately the film made at 100 watts has a very low deposition rate and it doesn't have as good of a crystallite thickness as those done at higher RF power. The film that has the best deposition rate, crystallite thickness, and peak intensity is the film grown at 250 watts. Actually the film grown at 250 watts would have the best characteristics of all the films if it wasn't for the residual stress in the film, because of this fact it was decided that we use this power setting and try to adjust the substrate temperature to see if we can relieve the stress in the film.

4.2.3 Substrate Temperature Effect

As was seen in the PLD system the temperature can have an effect on the film's interplanar spacing and therefore the residual stress. In the previous section the film grown at 250 watts had some of the best characteristics, and we will see later in the chapter it also has the best deposition rate making this power setting the most favorable, if it wasn't for the residual stress in the film. All of the temperature variations were done at 250 watts of power with the chamber pressure set at approximately 16 millitorr and with a 75:25 argon to oxygen flow rate. In the PLD system the residual stress in the films went from being a compressive stress at lower temperatures to a tensile stress at higher temperatures. It was believed that this would also hold true for the Sputtering system. Since the films grown in the Sputtering system showed a compressive stress at 200°C the

next step was to try making a deposition at a higher temperature to see if our conclusion is correct based on the PLD experiments. What can be seen from Table 4.6 is that it is in fact correct the film grown at 200°C had a compressive stress, the film grown at 300°C had less of a compressive stress and finally the film grown at 400°C had a slight tensile stress.

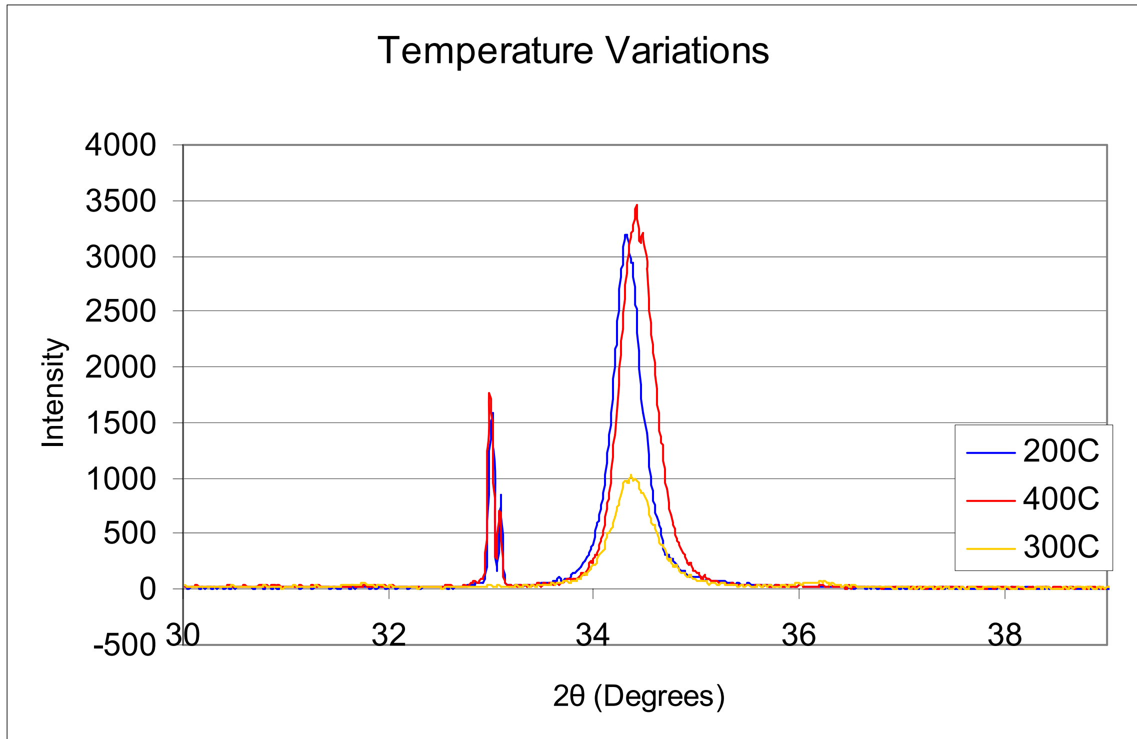

Figure 4.15 Temperature Variations

Table 4.8 XRD Analysis Based on Various Temperatures

Temperature (°C)	d_{002} (Å)	Crystallite thickness (nm)	2θ	σ (GPa)
ZnO Reference	2.60332	NA	34.422	NA
200	2.611828	26.52	34.31	-0.84038
300	2.607406	18.27	34.37	-0.40359
400	2.602999	21.645	34.43	0.031707

The prediction proved true, as can be seen in the above table and figure the residual stress did go down with the increase in substrate temperature. The film grown at 400°C is the best all around film grown, having the closest interplanar spacing to that of the reference value of ZnO, along with a good crystallite thickness, and deposition rate. This film has a single XRD peak position with good intensity, and when tested should give the best piezoelectric characteristics of all of the films grown.

The interesting thing that should be noted is that the sample grown at 300°C is polycrystalline. The typical XRD plots have the ZnO peak at around 34.4° with a little variation due to film stresses, and the XRD, occasionally picks up the silicon substrate producing a peak at 33°. The sample grown at 300°C has every ZnO peak possibility indicating that multiple crystal orientations are in the film. Figure 4.16 shows the XRD results of that sample.

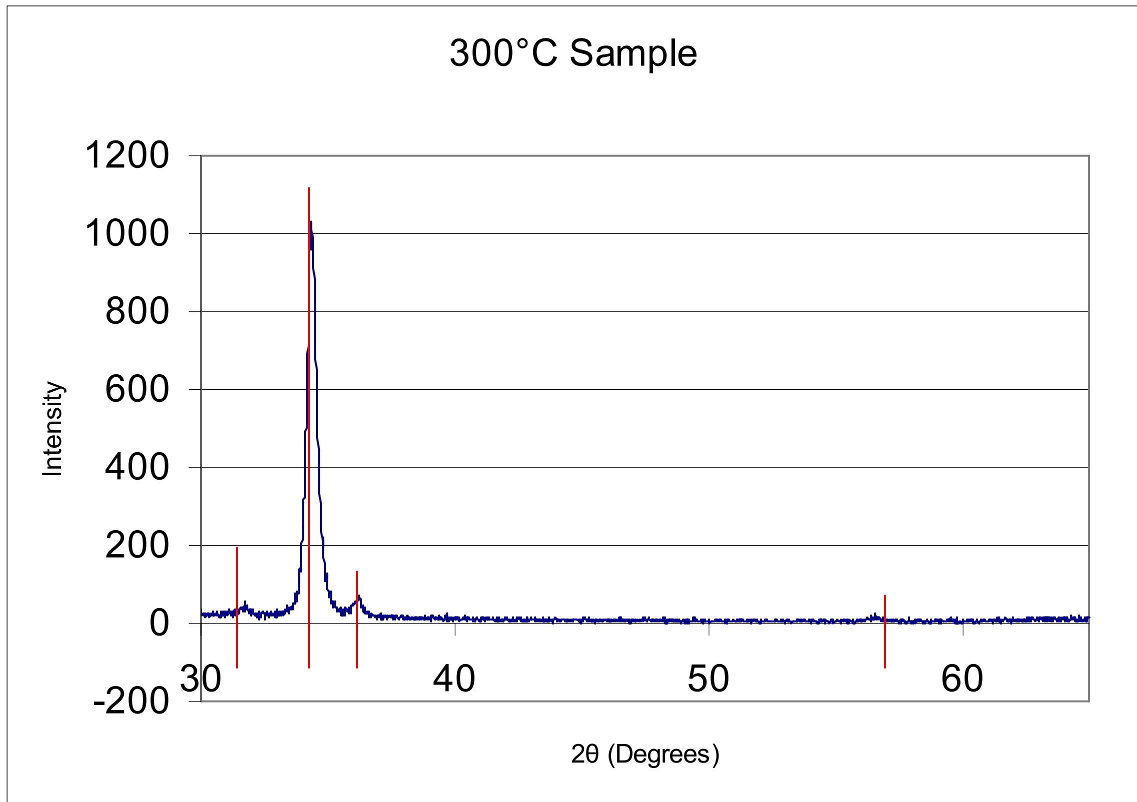

Figure 4.16 300°C Sample

The lines in Figure 4.17 show the different peak positions. The first peak occurs at around 32° representing the (100) orientation, the next one is at around 34.4° representing the (002) orientation, another peak occurs at around 36° showing the (101) orientation, and the last peak is at around 56.6° showing the (110) orientation. The reason why we get a polycrystalline film at 300°C and not at 200°C or 400°C is unclear, but the fact that this is what happens is probably why the peak is not as intense as the other two samples. When this film was analyzed by the XRD the initial thought was that something was wrong, so another film was grown at the same conditions and the same results were obtained. Thus leading to the conclusion that this was not a mistake and the film at 300°C is polycrystalline.

4.2.4 Roughness

The surface roughness of all of the thin films deposited by the sputtering method was characterized by the AFM. Figure 4.18 shows the roughness of the films grown on silicon (100) the x-axis is the RF power at which the films were grown on and the legend shows the substrates grown at different percent argon to oxygen flow rate and the substrates grown at the different temperatures.

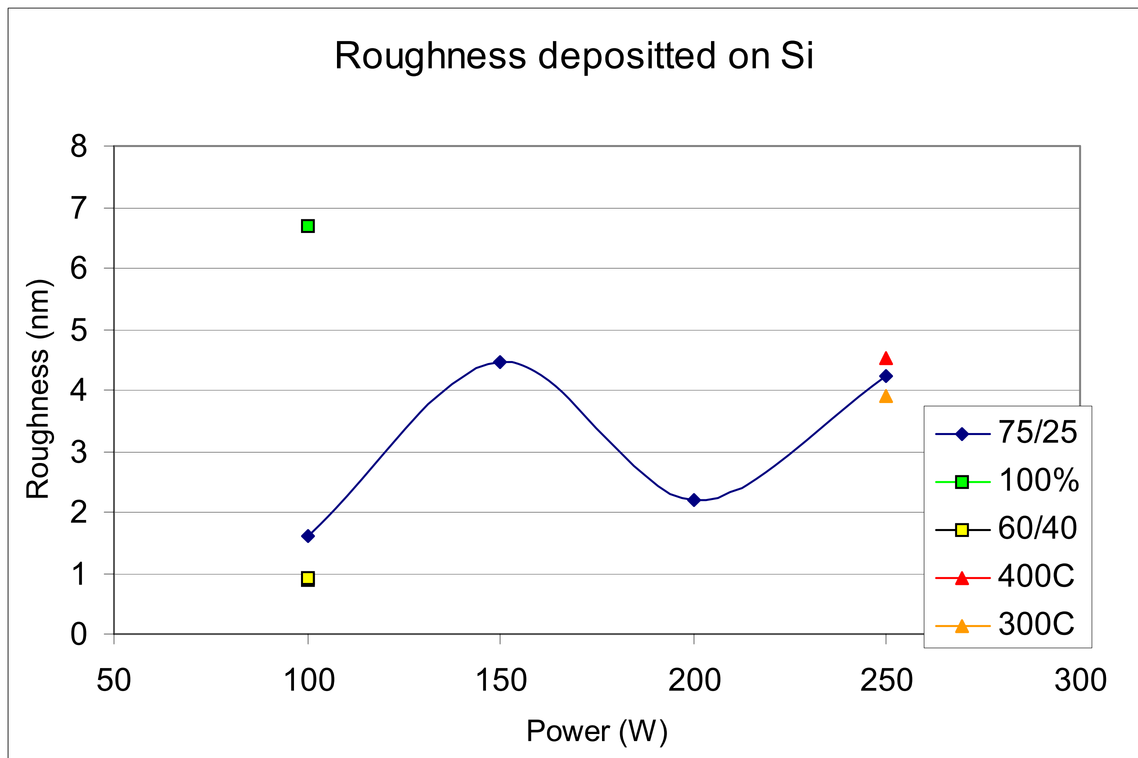

Figure 4.17 Sputtering Surface Roughness

4.2.5 Deposition Rate

To find the deposition rate of the sputtered samples, two samples were made one at 100 watts and one at 250 watts with a deposition time of 2.5 hours. These samples were masked with another piece of silicon to give a good stepping point, so the profilometer could be used to get an initial idea of what kind of deposition rates were achieved at both power extremes. After these two samples were characterized, the ellipsometer could be used to analyze the rest.

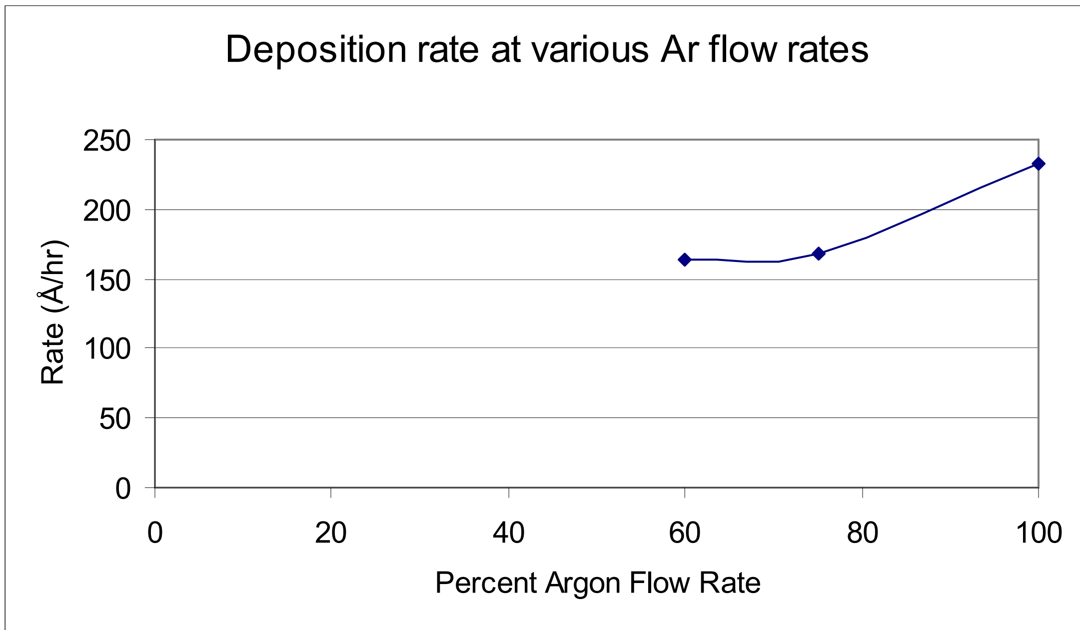

Figure 4.18 Deposition Rate at Various Ar % Flow Rates

Figure 4.19 shows the deposition rate of the films grown at different Ar:O_2 flow rates, these were the films discussed in section 4.2.1. The graph shows that the more argon in the chamber the better the deposition rate, which is what is to be expected. The more argon atoms that are ionized in the chamber and directed to the target, the more target atoms get sputtered off of the target. This graph confirms this.

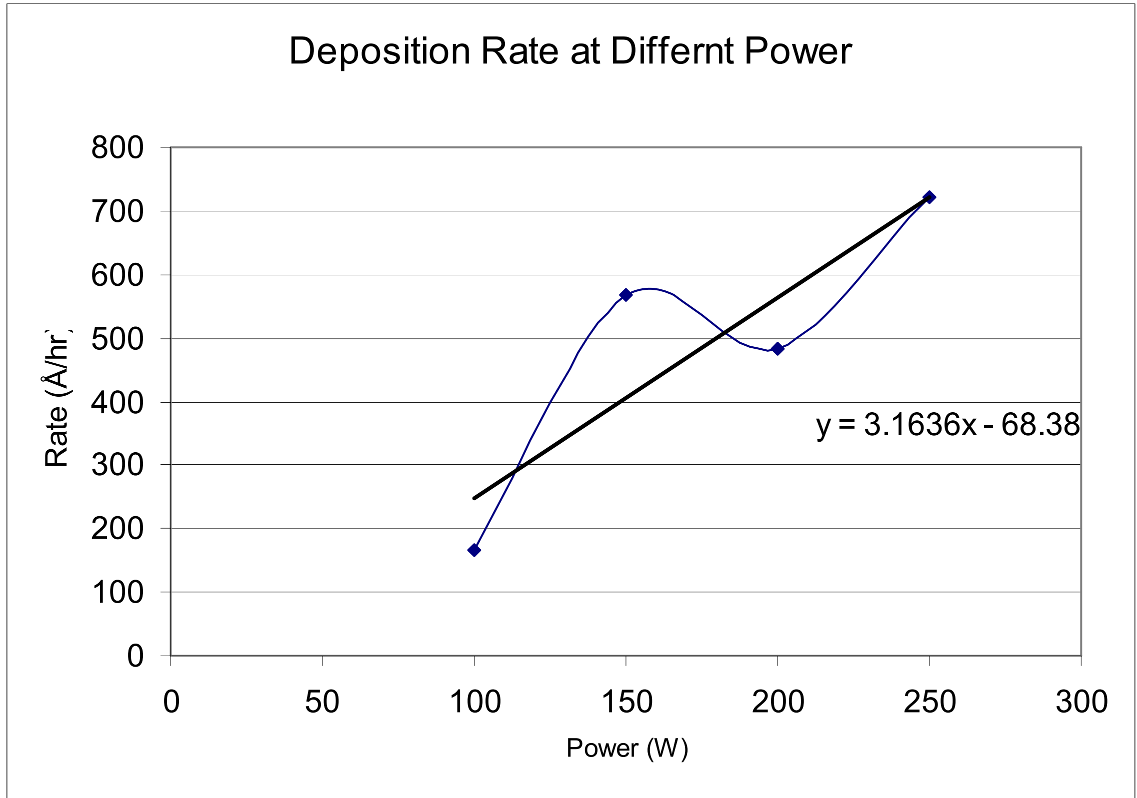

Figure 4.19 Deposition Rate at Different Power Settings

Figure 4.20 shows the deposition rate of ZnO at the different power settings of the films grown in section 4.2.2. A trend line was added to make it easier to see that the deposition rate increases with increasing power. Figure 4.20 gives a similar line as the roughness figure; it appears that a higher deposition rate or thicker film corresponds to a higher roughness.

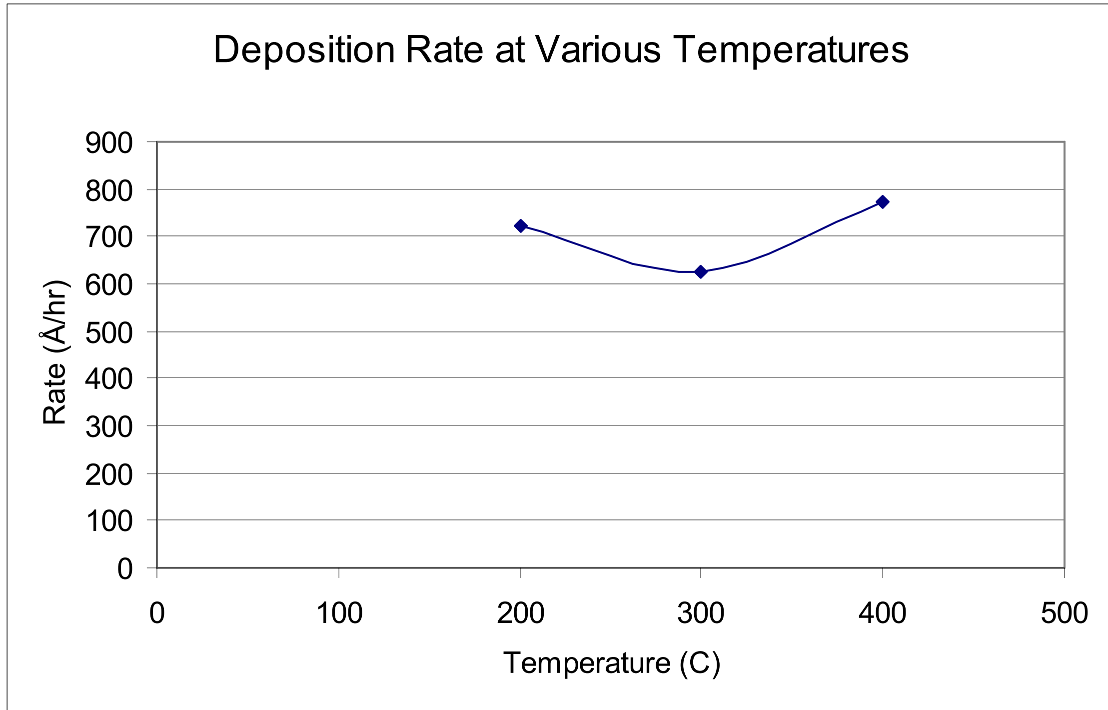

Figure 4.20 Deposition Rate at Various Temperatures

Figure 4.21 shows the films grown in section 4.2.3. The earlier PLD experiments showed that an increase in temperature gives an increase in deposition rate. This can be seen when comparing the 200°C and the 400°C sample to each other. The 300°C sample as was discussed in that section seemed to be polycrystalline forming differently than the other two samples, this could be the reason why it doesn't show the expected increase in deposition rate when compared to the lower temperature.

4.2.6 Conclusion of the Optimization of Sputtering Depositions

Many films were made at various deposition conditions to find the optimum "recipe" to grow a thin film. Other films may show better qualities when analyzed by any

one instrument, however, when taking the cumulative results this film is the best. The optimum condition for deposition is at 250 watts of RF power, 75% argon flowing through the chamber and 25% oxygen, and a substrate temperature of 400°C. This film showed the best XRD, AFM, and deposition rate.

4.3 Calculation of the Piezoelectric Coefficient by the Normal Load Method

For the calculation of the piezoelectric coefficient by the normal load method a system was constructed similar to K. Lefki and G.J.M Dormans system in there paper "Measurement of Piezoelectric Coefficient of Ferroelectric Thin Films [34]. The metal tip was $2.0mm^2$, and load was applied by dropping a 50 gram mass from a height of 50mm. A 0.1μF capacitor was put in parallel to the multimeter. Several samples were made by depositing ZnO onto a metal substrate, the metal substrate was used for two reasons one it acted like a bottom electrode and two when the load was applied the metal substrate wouldn't fracture like a silicon substrate would. The three samples that were made in this test were made in the sputtering chamber at the various temperatures just like in section 4.2.3. These samples were grown to get an approximate thickness of 200nm for every one of them. A piece of the bulk ZnO target material was also used; having a thickness of 1.0mm. Table 4.9 shows the calculated values.

Table 4.9 Piezoelectric Coefficients

	mgh (J)	*E* (N/mm^2)	V (mm^3)	*u* (J/mm^3)	σ_d (N/mm^2)	F (N)	Vc (mV)	d_{33} (pC/N)
ZnO Bulk	2.45 *10^{-2}	1.00 *10^5	4	6.13 *10^{-3}	3.50 *10^1	1.40 *10^2	5.37	4.29
ZnO Film	2.45 *10^{-2}	1.80 *10^5	0.0008	3.06 *10^1	3.32 *10^3	1.33 *10^4	0.16	0.0012

Table 4.9 shows the potential energy of the mass that was dropped from a height of 50mm, *E* is the modulus, and *V* is the volume of the ZnO material under the tip. From the known volume of ZnO material that gets strained and *u* strain energy density, a force *F* load can be determined and used to calculate the piezoelectric coefficient d_{33}.

The bulk ZnO shows a higher piezoelectric coefficient than the thin film, but not the true value for the d_{33} orientated film. The bulk target material shouldn't have the true value for the d_{33} since it does not have any specific crystal orientation, so when the ZnO was strained it was strained along a variety of orientations and not just along the axis that would obtain the d_{33} coefficient. As a result the d_{33} value of 12pC/N will never be obtained. However, a value on the same order of magnitude to any of the piezoelectric coefficients was obtained showing that the system did work fairly accurately.

Unfortunately the 300°C and the 400°C samples didn't produce any voltage or at least not enough for the multimeter to detect it. Since nothing was detected by these films they were not listed in the table. The 200°C, on the other hand, did produce enough of a voltage to calculate the piezoelectric response. The fact that the 200°C sample produced a voltage instead of the others proves that the bigger the crystallite thickness is, the better the piezoelectric property of the film is. Of course the fact that one of the thin films

worked versus the others could be due to experimental error, and given that the 200°C sample gave such a poor response indicates that their was a lot of error in the characterization of the piezo coefficient for all of the thin films. Some possible reasons for the error could be from the film thicknesses. The films made for this experiment had a thickness of 200nm, when the tip applied the force to the film it could have indented it or scratched it to the point where the tip penetrated the film some distance. This would give a different volume for the ZnO thin films and would alter the calculation, or the tip may have penetrated to the point of almost shorting out the circuit giving a low voltage. A thicker film deposited onto the metal substrates probably would have given better results. A thicker film would give a greater number of ZnO molecules in line with the load, when more molecules are strained more voltage could be produced.

Figure 4.23 shows the system used in the experiments, a mass is dropped through the tube in the center applying a force to the tip, which is resting on the substrate. The tip has a wire attached, which is attached to the capacitor, and the substrate rests on the aluminum tape, which is connected by a wire to the other side of the capacitor.

This experimental technique, at least with the equipment used, is prone to error, which could also be why the thin film samples never achieved the value of 12 pC/m like all other sources have listed as the piezoelectric coefficient. An example of a source for the error is the dropping of the mass. The impact of the mass depends on how consistently it is dropped from the given height; inconsistently dropping the mass would vary the force applied. Since no system has a 100% transfer of energy, when the mass impacts the tip some of the kinetic energy is changed into sound vibrations or lost to the environment through other reasons. However, even though the true value was never

obtained by the thin films, this test proves that the thin films produced a voltage when strained. Leading to the belief that with a better experimental set up, the actual valuse could be obtained.

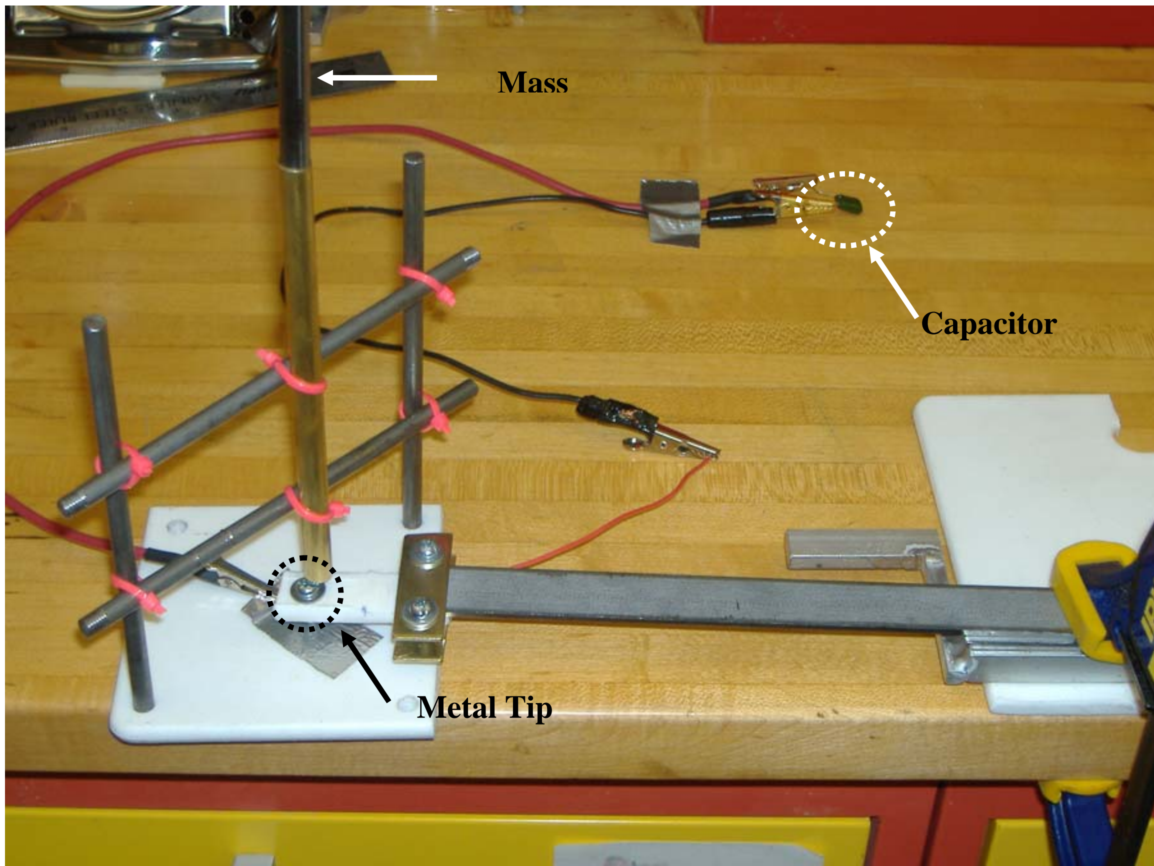

Figure 4.21 Experimental Equipment

CHAPTER FIVE: CONCLUSION AND FUTURE WORK

5.1 Conclusion

Many films were deposited by Pulsed Laser Deposition and Sputtering, these two techniques have many similarities in how they deposit films onto the substrate, how the temperature of the substrate affects the film, and how the addition of oxygen improves the oxide growth. The two techniques will be compared to give the pros and cons of the systems as well as the experimental results that were found at the various conditions.

Every system has its advantages and disadvantages; PLD has several advantages over sputtering and vice versa. The PLD system used in these experiments gave better deposition rates than the Sputtering system, to grow a thin film in the PLD system it might take 20 minutes to get a thickness of 200-300nm where as in the Sputtering system it would take about 5 hours to do achieve the same. Part of the reason for the difference in deposition rates is due to the fact that the PLD system has the substrate 40mm from the target where as the Sputtering system has it set at 80mm. The operation of the PLD system was also easier to use. Unfortunately, since this process relies on a laser beam to form the plasma, the plasma forms from the single point where the laser hits, creating a small plasma plume. Since the plume is relatively small, the system cannot deposit a uniform film over a large distance, so this is not a practical method for depositing on

large wafers. It did, however, allow us to examine the material properties of the film. And give us an understanding of the deposition parameters for ZnO.

The Sputtering system on the other hand, even though it is more complex to use and has a low deposition rate, will give a fairly uniform film. Part of the reason for the uniformity is because the substrate is rotated during the deposition. Another reason for the uniformity is how the plasma forms on the target. The RF power source used creates plasma over the entire target versus just a single point, and as a result creates a plasma plume with a bigger diameter.

For the deposition of ZnO regardless of which system is being used a certain amount of oxygen needs to be used in the system to get a good film. Even though both systems used a zinc oxide target, it was seen that the addition of extra oxygen in the chamber helped to ensure that the zinc ions formed with the oxygen ions on the substrate. However, too much oxygen in either system was as much of a detriment as not having enough. By having too much oxygen in the PLD chamber it reduced the mean free path in the system reducing deposition rates. For the Sputtering system, even though the total pressure in the system was held at 16 millitorr, having too much oxygen would reduce the number of argon atoms impacting the target, reducing the amount of zinc and oxygen atoms that are knocked off.

The deposition pressure used in either system varied drastically. The pressure in the PLD chamber produced decent films when the pressure was varied from 50-200 millitorr, a vast difference from the Sputtering pressure of 16 millitorr. Typically for both deposition techniques the lower the pressure is sought after because it gives the higher mean free path, and therefore a better deposition rate. For the PLD, since there was a

higher deposition rate, perhaps due to the close distance of the target and substrate, more oxygen was needed at any given time to make sure that the zinc had something to bond with on the substrates surface. When sputtering, less oxygen in the chamber was needed for the same reason that a lot of oxygen was needed in the PLD system. The lower deposition rate of the Sputtering system means that less zinc ions are reaching the target in a given amount of time requiring less oxygen at any given point in time to react with the zinc. Substrates grown in the PLD needed that significant amount of atoms to react with. It was at 200 millitorr were we reached the point were the extra oxygen got to be a significant detriment in reducing the mean free path and not helping the zinc to react any more.

The substrate temperature as mentioned in an earlier chapter gives the necessary energy to help in the formation of a crystalline film. When heat is added to the substrate a stress can form in the film due to a thermal expansion mismatch between the substrate and material being deposited. What holds true for both systems is that the stress formed in the system went from a compressive stress at lower temperatures to a tensile stress at higher temperatures. An interesting find is that the temperature where the film goes from a compressive to a tensile stress is different in each system. In the PLD the stress became tensile at around 200°C, in the Sputtering system this didn't happen until about 400°C.

The surface roughness is another characteristic that was analyzed in all of the films. When comparing the roughness between the two systems we see that the results are very similar. When a decent amount of oxygen was in the chamber and the temperature was in the 200°C to 400°C range the roughness was somewhere around 4-6 nm. From this result it looks that the deposition rate had no effect on the roughness. The lack of

oxygen in the PLD chamber produces lower roughness films where as the opposite is true for the Sputtering system, a 100% argon atmosphere gives a higher roughness.

The results, advantages, and disadvantages of both systems were discussed, but in the end neither system is completely superior to the other. The characteristics of each system makes them useful in different ways. The bottom line is that the machine and the experimental conditions of the deposition depend on the use of the material being deposited. To grow a thick film, it makes sense to use the PLD since it had a good deposition rate. The PLD made it easy to characterize the films quickly to get a basic understanding of zinc oxide. The Sputtering system on the other hand is the better system to use for depositing a uniform film over a bigger area.

5.2 Piezoelectric Response with the AFM

So far most of the work in this thesis has been characterizing the films interplanar spacing, roughness, thickness, and mechanical characteristics. The first part of the research has been finding the best deposition conditions to get the listed results; the next step is to really focus on obtaining the best piezoelectric properties. As mentioned before some measurements were done using the normal load method; however more accurate measurements can be obtained by using the AFM. This method uses the inverse piezoelectric effect for the measurements. A voltage is passed through the sample at a frequency of about 500Hz, causing the film to strain. The strain can be picked up by the

AFM tip, and based on the voltage applied and the amount of deformation in the film the piezoelectric coefficient can be calculated.

An initial measurement was done on the 400°C sample to see if the film responded. A voltage was passed through the sample ranging from zero to five volts at a frequency of 500Hz. A few AFM pictures were captured showing that the film did respond to the applied voltage. This sample is the same sample tested in the normal load method. Using the normal load method the sample didn't have any response, but by using the AFM we could probe a smaller area of our choosing, seeing a more localized response. Figure 5.1 shows the images obtained from the AFM.

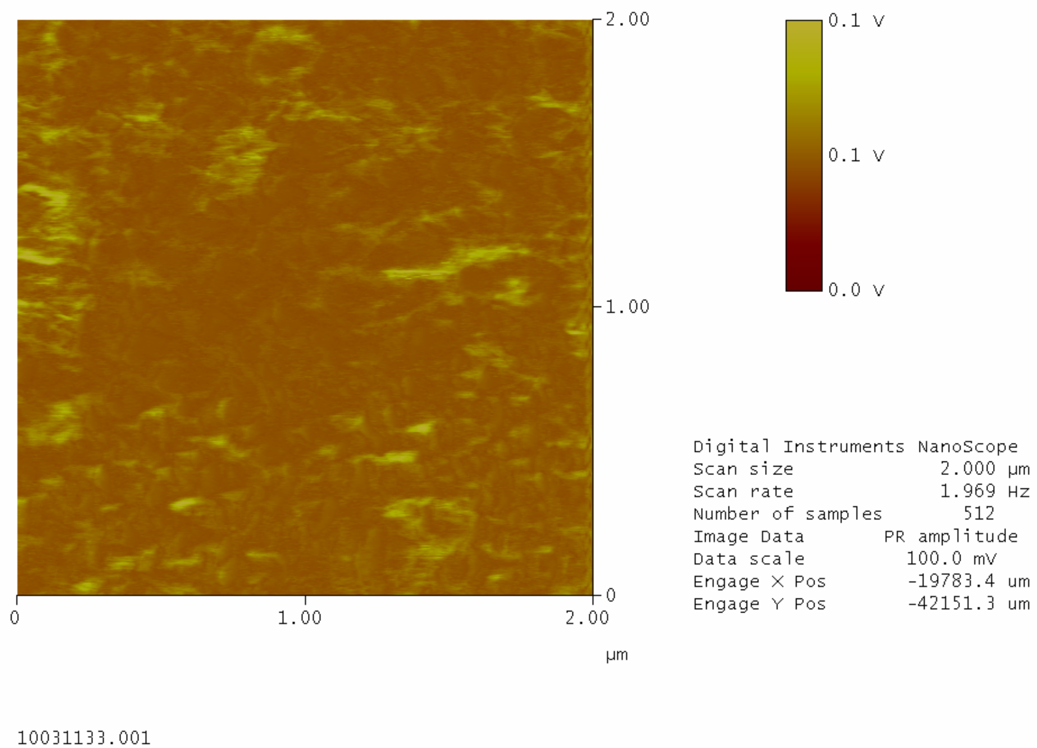

Figure 5.1 AFM Results of Films Piezoelectric Effect

According to the Piezo Response manual from Veeco, “The PR amplitude data will appear only on regions of the surface that are in plane with the sample surface. This is because the PR amplitude is a function of the sample moving the tip up and down. Areas that are not in plane will not move the tip.” [28]

Finding the Piezo Response (PR) with the AFM is listed in the future works section because only one sample was used in the instrument, and that sample was done to learn how to set up the equipment for the measurement and how the software works. Many more samples should be tested in order to find the best results for making a cantilever resonator.

5.3 Resonator

Once the piezoelectric properties were analyzed at the different experimental conditions, a resonator can then be made with the optimum film. Some initial modeling was done in Coventor. Coventor was used to find the first two modes of vibration in the beam. A cantilever bean was made with a top and bottom electrode made of platinum and a center layer of zinc oxide. The beam is 10µm wide and 100µm long and the layer thicknesses are listed in table 1.2. Figures 5.2 and 5.3 illustrate the first two modes of vibration. The first mode of vibration occurs at a frequency of 451.4kHz and the second mode of vibration occurs at 1.24MHz.

The next future step would be to actually build a cantilever resonator like the one modeled in Coventor and then test it. The testing process would involve rechecking the

piezoelectric response of the ZnO used in the cantilever beam by applying a voltage to the top and bottom electrode at a frequency, and then optically observing the strain due to the voltage. Once again knowing the voltage and measuring the strain we can find the piezoelectric coefficient. The resonant frequencies that Coventor found can also be tested by applying a voltage at those frequencies. At that point we can see how close the model is to reality.

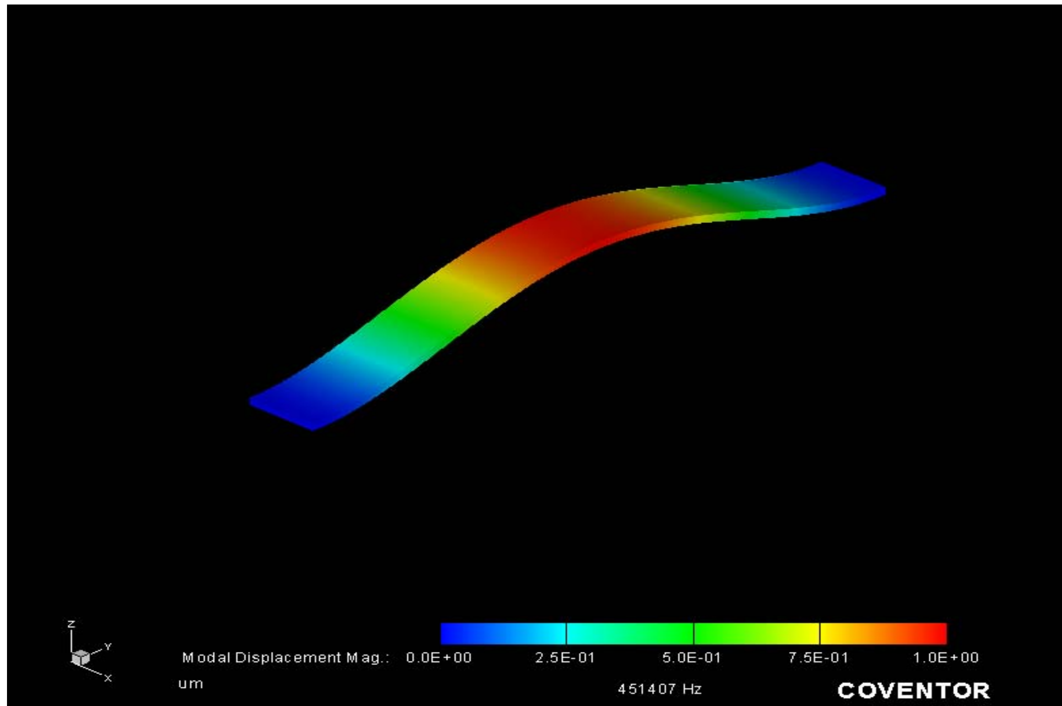

Figure 5.2 First Mode of Vibration

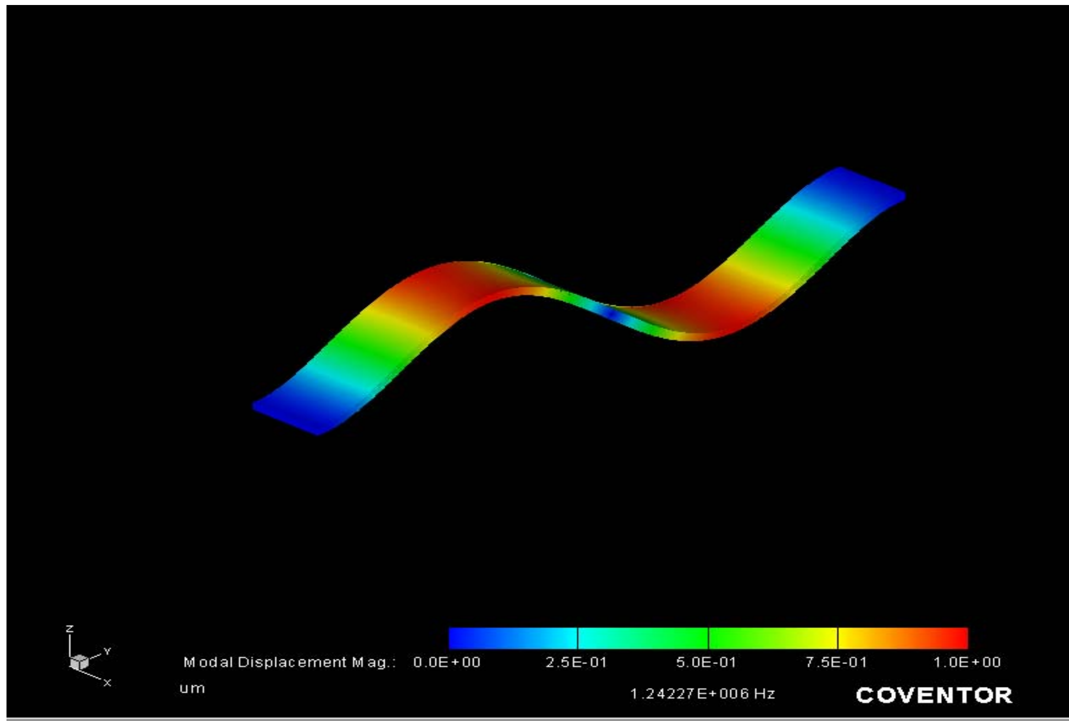

Figure 5.3 Second Mode of Vibration

5.4 Future of the Field

Since the work in this thesis has been the analysis of ZnO thin films and the use of it in a resonator, I would also like to include a section describing where the field itself is leading to and the importance of using zinc oxide films. MEMS systems are currently being used in every day life, beam resonators to date have been used in a variety of applications including frequency generators, filters, and sensors. Another use for these structures, which I believe hasn't been fully analyzed or at least has a lot of room for improvement is the use of these structures for scavenging energy from the vibration of materials. Article in Vol. 171, No. 22 of Science News mentions how piezoelectric

materials can be used to do this. By vibrating the piezoelectric material voltage can be produced, this voltage could then by used to power circuitry. The future of the field would be to create sensors that get their power internally from the vibrations of its environment.

An example mentioned in this article was to make a sensor that could be used on helicopter blades to get information on fatigue. The sensor would then determine when the blade would need to be replaced, making the operation of the helicopter safer. By using a resonator with a piezoelectric material and integrating it onto the sensor, the sensor would run on the vibrations produced by the rotation of the blades in flight. No wires to and from the sensor would be required, and of course in something like a helicopter, commercial, or military aircraft there are hundreds to thousands of sensors all currently requiring wires to them [35]. So by implementing a wireless sensor, at least in aviation, would mean less weight on the aircraft and as a result less fuel burn.

The use of zinc oxide as a resonator is just one of the applications in the MEMS devices; a further step in making things smaller would be to use it in the nano world. Zinc oxide can create a number of nanostructures including nanowires, nanowire arrays, nanotube, and the list goes on. Just like what was mentioned above in scavenging energy from the environment, nanowire arrays could be used to power nanodevices. Aside from just its piezoelectric effect zinc oxide nanorods could one day be used as an ultraviolet laser [7].

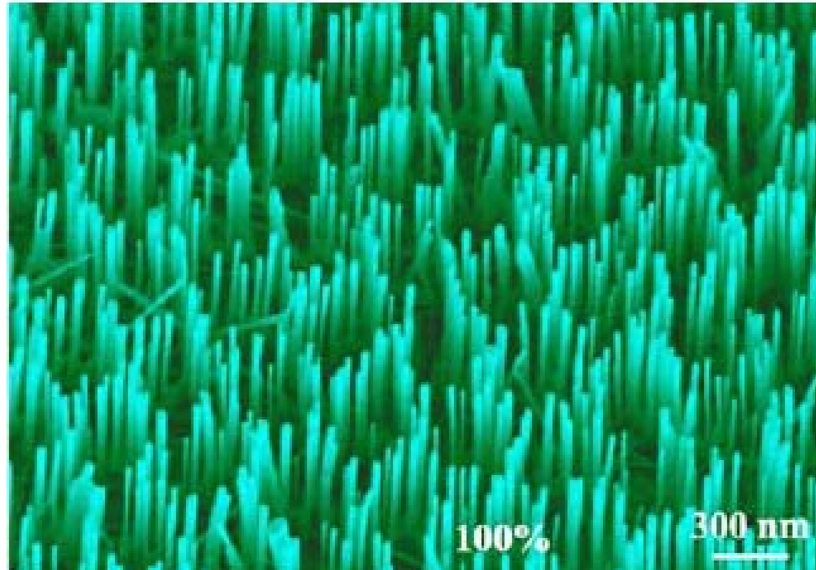

Figure 5.4 ZnO Nanowire Array

As can be seen ZnO has a number of applications, making it a very versatile material. It has already made its way into MEMS devices and its nano characteristics and uses are continuing to be explored. There is a lot of potential for zinc oxide, and other uses for this material will continue to be discovered.

REFERENCES

[1] S. Vicknesh, S. Tripathy, V.K.X. Lin, S.J. Chua B. Kumar, and H. Gong, Surface Micromachined Freestanding ZnO Microbridge and Cantilever Structures on Si(111) Substrates", Applied Physics Letters 90, 091913 (2007).

[2] B. Piekarski, D. DeVoe, M. Dubey, R. Kaul, J. Conrad, and R. Zeto, Surface Micromachined Piezoelectric Resonant Beam Filter, U.S. Army Research Laboratory, University of Maryland College Park.

[3] S. Kadlec, E. Kugler, and S. Krassnitzer, Very High Uniformity Single-wafer Physical Vapor Deposition Processing of Piezoelectric Films for Bulk Acoustic Wave Devices, Business Briefing: Global Semiconductor Manufacturing Technology (2003).

[4] Linh Mai, Dong-Hyun Kim, Munhyuk Yim, and Giwan Yoon, A Feasibility Study of ZnO-Based FBAR Devices for an Ultra-Mass-Sensitive Sensor Application, Microwave and Optical Technology Letters Vol. 42, No. 6, pp. 505-507 (2004).

[5] N. Staszkiewicz, Synthesis and Characteristics of ZnO Nanowires, NNIN Research Accomplishments, pp. 132-133 (2004).

[6] Ying Dai, Yue Zhang, Yuan Qiang Bai, and Zhong Lin Wang, Bicrystalline zinc oxide Nanowires, Elsevier, Chemical Physics Letters (2003).

[7] M. Telford, Making ZnO Nanorods the Cool Way, Materials Today p.13, (2005).

[8] Z.L. Wang, Novel Nanostructures of ZnO for Nanoscale Photonics, Optoelectronics, Piezoelectricity, and Sensing", Applied Physics A (2007).

[9] Z. L. Wang, and J. Song, Piezoelectric Nanogenerators Based on Zinc Oxide Nanowire Arrays, Science Vol. 312, pp.242-245, www.sciencemag.org, (2006).

[10] Raegan Lynn Johnson, Characterization of Piezoelectric ZnO Thin Films and the Fabrication of Piezoelectric Micro-Cantilevers", Masters Thesis, Iowa State University, Ames Iowa (2005).

[11] Shweta Humad, Piezo-on-Silicon Microelectromechanical Resonators, Masters Thesis, Georgia Institute of Technology (2004).

[12] William L. Hughes, Synthesis and Characterization of Zinc Oxide Nanostructures for Piezoelectric Applications, Doctoral Thesis, Georgia Institute of Technology (2006).

[13] Baomin Xu, Piezoelectric Materials and Devices, Palo Alto Research Center Inc., Palo Alto (2003).

[14] Yolanda Y. Villanueva, Da-Ren Liu, and Pei Tzu Cheng, Pulsed Laser Deposition of Zinc Oxide, Ateneo de manila University and Precision Instrument Development Center (2005).

[15] Amanda Allison Frederick, Analysis and Fabrication of MEMS Tunable Piezoelectric Resonators, Masters Thesis, University of Pittsburgh (2006).

[16] Shweta Humad, Reza Abdolvand, Gavin K. Ho, Gianluca Piazza, and Farrokh Ayazi, High Frequency Micromechanical Piezo-on-Silicon Block Resonator, IEEE (2003).

[17] Gianluca Piazza, Philip J. Stephanou, and Albert P. Pisano, Piezoelectric Aluminum Nitride Vibrating Contour-Mode MEMS Resonators, IEEE (2006).

[18] Johan Bohlmark, Fundamentals of High Power Impulse Magnetron Sputtering, Institute of Technology, Linkoping University.

[19] Patrick Wellenius, Nitrogen Doping and Ion Beam Processing of Zinc Oxide Thin Films, Masters Thesis, Raleigh NC (2005).

[20] P. Verardi, and M. Dinescu, Characteristics of ZnO Thin Film Transducers Deposited by Pulsed Laser Deposition, IEEE Ultrasonics Symposium (1995).

[21] T.K. Subramanyam, B. Srinivasulu Naidu, S. Uthanna, Physical Properties of Zinc Oxide Films Prepared by DC Reactive Magnetron Sputtering at Different Sputtering Pressures, Sri Venkateswara University and Technical University of Munich (2000).

[22] Craig R. Barrett, William D. Nix, Alan S. Tetelman, The Principles of Engineering Materials, Prentice-Hall, Inc. (1973).

[23] Wesley Tennyson, X-Ray Diffraction, NanoLab/NSF Nue/Bumm.

[24] R. N. Tait and A. Mirfazli, Low Temperature Aluminum Nitride Deposition on Aluminum by RF Reactive Sputtering, American Vacuum Society, J, Vac Sci. Technol. A (2001).

[25] H.R. Zeng, H.F. Yu, S.X. Hui, R.Q. Chu, G.R. Li H.S. Luo, and Q.R. Yin, Local Elasticity Imaging of Ferroelectric Domains in $Pb(Mg_{1/3}Nb_{2/3})O_3$-$PbTiO_3$ Single Crystals by Low-Frequency Atomic Force Acoustic Microscopy, Elsevier, Solid State Communications (2005).

[26] Atomic Force Microscope Short User Gude.

[27] A. Petraru, V. Nagarajan, H. Kohlstedt, R. Ramesh, D.G. Scholm, and R. Waser, Simultaneous Measurement of the Piezoelectric Ferroelectric Capacitors by an Atomic Force Microscopy Based Approach, Appl. Phys. A 84, pp. 67-71 (2006).

[28] Piezo Response, Veeco.

[29] Piezoresponse Imaging, Veeco.

[30] Desheng Fu, Kazuyuki Suzuki, and Kazumi Kato, Piezoelectric Properties of $CaBi_4Ti_4O_4$ Ferroelectric Thin Films Investigated by Atomic Force Microscopy, The Japan Society of Applied Physics, Vol. 42, pp. 5994-5997 (2003).

[31] Anthony C. Fischer-Cripps, Nanoindentation, Springer-Veriag New York, Inc. (2002).

[32] Han-Ki Yoon and Yun-Sik Yu, Hardness and Elastic Modulus of ZnO Deposited Materials by PLD Method, IEEE (2005).

[33] Donald L. Smith, Thin-Film Deposition Principles and Practice, McGraw-Hiull, Inc. (1995).

[34] K. Lefki, and G.J.M. Dormans, Measurement of Piezoelectric Coefficient of Ferroelectric Thin Films, American Institute of Applied Physics, J. Appl. Phys. 76 (1994).

[35] M. Mitchell Waldrop, Powering the Revolution, Science News, Vol. 171, No. 22, pp. 344-345, 348 (2007).